Validation of ATR FT-IR to identify polymers of plastic marine debris, including those ingested by marine organisms

Melissa R. Jung[a], F. David Horgen[a], Sara V. Orski[b], Viviana Rodriguez C.[b], Kathryn L. Beers[b], George H. Balazs[c], T. Todd Jones[c], Thierry M. Work[d], Kayla C. Brignac [e], Sarah-Jeanne Royer [f], K. David Hyrenbach[a], Brenda A. Jensen[a], and Jennifer M. Lynch[g]

[a]College of Natural and Computational Sciences, Hawai'i Pacific University, Kaneohe, HI, United States

[b]Materials Science and Engineering Division, National Institute of Standards and Technology, Gaithersburg, Maryland 20899, United States

[c]Pacific Islands Fisheries Science Center, National Marine Fisheries Service, Honolulu, HI, United States

[d]U.S. Geological Survey, National Wildlife Health Center, Honolulu Field Station, Honolulu, HI, United States

[e]School of Ocean, Earth Science, and Technology, University of Hawai'i at Manoa, Honolulu, HI, United States

[f]Daniel K. Inouye Center for Microbial Oceanography: Research and Education, University of Hawai'i at Manoa, Honolulu, HI, United States

[g]Chemical Sciences Division, National Institute of Standards and Technology, Kaneohe, HI, United States

Corresponding author:

Jennifer M. Lynch
Chemical Sciences Division, National Institute of Standards and Technology, 45-045 Kamehameha Hwy, Kaneohe, HI, United States
jennifer.lynch@nist.gov 843-442-2188

ABSTRACT

Polymer identification of plastic marine debris can help identify its sources, degradation, and fate. We optimized and validated a fast, simple, and accessible technique, attenuated total reflectance Fourier transform infrared spectroscopy (ATR FT-IR), to identify polymers contained in plastic ingested by sea turtles. Spectra of consumer good items with known resin identification codes #1-6 and several #7 plastics were compared to standard and raw manufactured polymers. High temperature size exclusion chromatography measurements confirmed ATR FT-IR could differentiate these polymers. High-density (HDPE) and low-density polyethylene (LDPE) discrimination is challenging but a clear step-by-step guide is provided that identified 78 % of ingested PE samples. The optimal cleaning methods consisted of wiping ingested pieces with water or cutting. Of 828 ingested plastics pieces from 50 Pacific sea turtles, 96 % were identified by ATR FT-IR as HDPE, LDPE, unknown PE, polypropylene (PP), PE and PP mixtures, polystyrene, polyvinyl chloride, and nylon.

KEYWORDS

Sea turtles; Pacific Ocean; Marine plastic debris; Plastic ingestion; Fourier transform infrared spectroscopy; Polymer identification

1. Introduction

Plastic is one of the most persistent and abundant types of marine debris (Rios et al., 2007). For instance, high concentrations of up to 334, 271 pieces/km^2 have been estimated floating in the North Pacific central gyre, where this material is concentrated by wind-driven ocean currents (Moore et al., 2001; Howell et al., 2012). The production of plastic and associated marine plastic debris continues to rise (Geyer et al., 2017; Jambeck et al., 2015; Bakir et al., 2014; Hoarau et al., 2014), with an estimated 4.8 million metric tons to 12.7 million metric tons of plastic debris entering the marine environment each year (Jambeck et al., 2015). As marine plastic debris continues to accumulate, long-term environmental, economic, and waste management problems grow, including significant economic costs for prevention and clean-up (Singh & Sharma, 2008; Mcllgorm et al., 2011). Increasing awareness of the possible ecological impacts of marine debris has stimulated research to quantify and understand the incidence and magnitude of plastic ingestion by marine animals (Andrady, 2011; Provencher et al., 2017).

Ingestion of plastic debris has been documented in marine species across a range of sizes and biological complexity: from microscopic zooplankton to large vertebrates (Hoss and Settle, 1990; Nelms et al., 2015; Cole and Galloway, 2015; Unger et al., 2016). The size of ingested plastic debris occupies a large range, evidenced by filter feeders, like oyster larvae, which can ingest microplastics as small as 0.16 µm diameter (Cole & Galloway, 2015), while large items such as part of a car engine cover (650 mm x 235 mm) have been found in the gastrointestinal tracts of sperm whales (*Physeter macrocephalus*) (Unger et al., 2016). Sea turtles are a good indicator of plastic debris occurrence in the natural environment as studies have documented ingestion around the

74 world including coastal Florida, southern Brazil, the Central Pacific, and Mediterranean
75 Sea (Bjorndal et al., 1994; Bugoni et al., 2011; Clukey et al., 2017; Tomas et al., 2002).
76 Sea turtles ingest a variety of plastic items of varying types, sizes, and morphologies,
77 including pieces of bags, rope, fishing line, foam, and fragments of less flexible plastic
78 that range in size from microplastics (<5 mm on largest edge) to macroplastics (>25 mm)
79 with fragments up to 10 cm observed (Bugoni et al., 2001; Tomas et al., 2002; Clukey et
80 al., 2017). A study by Clukey et al. (2017) showed that a total of 2,880 plastic debris
81 items were ingested by 37 olive ridley (*Lepidochelys olivacea*), nine green (*Chelonia*
82 *mydas*), and four loggerhead (*Caretta caretta*) pelagic sea turtles that were incidentally
83 taken by longline fisheries in the North Pacific Ocean. Plastic fragments constituted 79.5
84 % of the total debris while 12.5 % were thin plastic sheets (e.g., bags and thin packaging
85 material) and 6.1 % were line or rope (Clukey et al., 2017). While the commercial use of
86 some ingested plastics, such as bags and fishing line, can be easily identified by visual
87 inspection, few pieces are found completely intact and their original origin is difficult to
88 discern (Hoss & Settle, 1990). Fortunately, plastic manufacturers and standards
89 organizations have developed a standard identification system for general classes of
90 plastic that can be used to help identify their likely intended commercial use.
91 Most plastic consumer goods are labeled with standardized resin codes marked
92 inside a triangle (ASTM, 2013), signifying the chemical composition of the main
93 polymer, which is used to sort and recycle compatible materials. These include
94 polyethylene terephthalate (PETE, #1), high-density polyethylene (HDPE, #2), polyvinyl
95 chloride (PVC, #3), low-density polyethylene (LDPE, #4, which also currently includes
96 linear LDPE [LLDPE]), polypropylene (PP, #5), polystyrene (PS, #6), and other

97 polymers (#7). These codes are rarely present or legible in recovered plastic debris or
98 small plastic fragments, hence identification of the polymer must be accomplished using
99 chemical testing. Characterizing unknown polymers helps illuminate many of the issues
100 surrounding marine debris. Knowing the polymer structure will aid in determining the
101 transport and fate of debris pieces in the environment, such as the effect of material
102 density on stratification within the water column or the susceptibility of specific chemical
103 bonds to break under environmental conditions. In addition, different polymers have
104 different affinities for adsorbing chemical pollutants from seawater, suggesting some
105 polymers may present a larger risk of transferring pollutants to marine organisms who
106 ingest them (Rochman et al., 2013, Fries and Zarfl, 2012; Endo et al., 2005; Koelmans et
107 al., 2013). Knowing the predominant polymers found in various habitats or ingested by
108 marine organisms can help focus conservation efforts, including changes to recycling
109 strategies, targeted waste management, or novel approaches in polymer production (Ryan
110 et al., 2009). Furthermore, since certain polymers are more commonly recycled than
111 others (e.g., #2 HDPE compared to #4 LDPE), it is important to be able to distinguish
112 these among debris to monitor the success of waste management techniques.
113 Several analytical tools have been used to identify the composition of plastic
114 debris (Andrady, 2017). For example, environmental samples from German rivers were
115 analyzed using thermogravimetric analysis connected to solid-phase adsorbers that were
116 subsequently analyzed by thermal desorption gas chromatography mass spectrometry
117 (GC/MS; Dümichen et al., 2015). Fisher & Scholz-Bottcher (2017) used pyrolysis-
118 GC/MS to identify microplastics ingested by North Sea fish. In addition, GC/MS has
119 been utilized to identify indicator chemicals characteristic of different polymers of

120 plastics ingested by Laysan albatross (*Phoebastria immutabilis*) (Nilsen et al., 2014).
121 These methods are limited to only volatile or ionizable compounds, such as small
122 oligomeric fragments or additives within the bulk material. Methods that can analyze the
123 entire sample, and often require less sample preparation, are vibrational spectroscopy
124 measurements such as Raman micro-spectroscopy (Frère et al., 2016) and Fourier
125 transform infrared (FT-IR) spectroscopy. FT-IR is becoming the most common technique
126 for marine debris polymer identification. It has been used to identify microplastics near
127 the surface of the Ross Sea, from the English Channel, and ingested by zooplankton
128 (Cincinelli et al., 2017; Cole et al., 2014). Recently, Mecozzi et al. (2016) used FT-IR
129 coupled with the Independent Component Analysis (ICA) database and Mahalanobis
130 Distance (MD) to identify marine plastics ingested by four loggerhead sea turtles in the
131 Mediterranean Sea.
132 FT-IR spectroscopy offers a simple, efficient, and non-destructive method for
133 identifying and distinguishing most plastic polymers, based on well-known infrared
134 absorption bands representing distinct chemical functionalities present in the material
135 (Verleye et al., 2001; Coates, 2000; Asensio et al., 2009; Beltran & Marcilla, 1997; Noda
136 et al., 2007; Nishikida & Coates, 2003; Iharco & Barros 2000; Guidelli et al., 2011;
137 Rotter & Ishida, 1992; Asefnejad et al., 2011). Structural isomeric polymers, such as
138 HDPE and LDPE, are difficult, yet important, to differentiate. Asensio et al. (2009) and
139 Nishikida & Coates (2003) reported that LDPE had a unique characteristic (yet quite
140 small) band at 1377 cm^{-1}, representing a CH_3 bending deformation, suggesting that even
141 these similar polymers can be distinguished using FT-IR spectra. This band is reportedly
142 absent in HDPE. These polymers differ by the extent of branching with HDPE being a

143 linear PE chain with minimal branching, LLDPE having short alkyl branches off a linear
144 backbone, and LDPE having long PE branches that represent a significant portion of the
145 total chain length. Increased branching will reduce material density, with HDPE densities
146 ranging from 0.94 g/mL to 0.97 g/mL and LLDPE and LDPE densities ranging from 0.90
147 g/mL to 0.94 g/mL (Peacock, 2000; Verleye et al., 2001). However, chemical weathering,
148 natural aging, and biochemical processes affecting ingested plastics can modify their
149 spectral features, making identification difficult (Mecozzi et al., 2016), which was
150 evident in Brandon et al. (2016) in which 30 % of marine debris polyethylene (PE)
151 samples could not be differentiated. These particularly challenging pieces produce
152 confusing spectra due to the similar intensities of bands at 1377 cm^{-1} and 1368 cm^{-1}. No
153 study has yet tested or provided criteria on how to differentiate these.
154 The goal of this study was to thoroughly assess the validity of attenuated total
155 reflectance (ATR) FT-IR for identifying polymer composition of ingested plastic marine
156 debris. This chemical technique is certainly not new and is common, but our study
157 provides novel details that can help future studies avoid pitfalls, reduce confusion, and
158 increase identification accuracy. We provide a clear guide with strict criteria to
159 differentiate spectra from HDPE and LDPE. Furthermore, we identified and described the
160 most effective cleaning method for preparing ingested plastic samples of three common
161 polymers from pelagic, long-line caught olive ridley sea turtles to obtain high quality
162 spectra. Sample handling was minimized to retain the original sample in a specimen bank
163 for future additional chemical testing. To accomplish these goals, we developed an in-
164 house spectral library from plastic consumer goods marked with resin codes. We
165 validated our library with polymers originating from National Institute of Standards and

Technology (NIST) Standard Reference Materials (SRMs) ®, polymer standards obtained from scientific vendors, raw polymers sourced from manufacturers, and an additional set of consumer goods with polymer identity unknown to the analyst. PE materials of known density were used to confirm that ATR FT-IR is capable of discriminating between HDPE and LDPE, and to determine if a float/sink test in various dilutions of ethanol could further assist in differentiating these polymers. Using these optimized ATR FT-IR methods, we analyzed 828 ingested plastic items for polymer identity. A subset of these ingested samples was analyzed at NIST using high temperature size exclusion chromatography (HT-SEC) to confirm the accuracy of polymer identification by ATR FT-IR.

2. Methods

2.1. Plastic Standards

Plastic standards were obtained from four sources with different degrees of purity or certainty (See Supplemental Material Table S1 for a complete list). Four NIST SRMs and 10 polymers that were sourced from scientific/laboratory vendors (scientifically sourced) were considered the purest or best characterized. Raw materials obtained from manufacturers were considered purer than the consumer goods collected, which could contain additives. These standards represent each resin code #1 through #6, LLDPE, and several code #7 or other polymers (Table S1). The #7 category included polymers that could be found in marine debris, including acrylonitrile butadiene styrene (ABS), cellulose acetate (CA), ethylene vinyl acetate (EVA), latex, nitrile, nylon (represented by nylon 12 and nylon 6,6), polycarbonate (PC), poly(methyl methacrylate) (PMMA or

190 acrylic), polytetrafluoroethylene (PTFE), fluorinated ethylene propylene (FEP), and
191 polyurethane (PU).
192 Two to three consumer goods or raw materials labeled with each resin code were
193 used to create standard spectra for each polymer. While consumer goods likely contain
194 additives, the in-house spectral library was intentionally based on spectra from consumer
195 goods, because they were assumed to more closely represent consumer items found in
196 marine debris and ingested by marine organisms.
197 To validate the polymer identification by the analyst from ATR FT-IR spectra,
198 eleven additional consumer goods with stamped resin codes were used in a blind test
199 (Table S1): PETE (n=2), HDPE (n=3), LDPE (n=2), PE of unknown density (n=1), PP
200 (n=2), and PS (n=1).
201
202 *2.2. ATR FT-IR Instrument Details*
203
204 A Perkin Elmer FT-IR Spectrometer Spectrum Two Universal ATR was used to
205 collect spectra from 4000 cm^{-1} to 450 cm^{-1} with a data interval of 1 cm^{-1}. Resolution was
206 set at 4 cm^{-1}. The ATR diamond crystal was cleaned with 70 % 2-propanol and a
207 background scan was performed between each sample. Each sample was compressed
208 against the diamond with a force of at least 80 N to ensure good contact between sample
209 and ATR crystal, as recommended by Perkin Elmer. Absorption bands identified using a
210 peak height algorithm within the Perkin Elmer software were recorded and compared to
211 absorption bands of each polymer reported in the literature and obtained from our in-
212 house spectral library (Tables 1 and 2). A minimum of four matching absorption bands
213 were required for accepted identification. Spectra of consumer goods of each polymer
214 type tested are shown in Figure 1. No pre-existing spectral library or database was used in

this study. This was intentional, because comprehensive libraries can be expensive. We wanted out approach to be available to all labs regardless of their resources. Secondly, relying solely on automated library searches and statistical methods can lead to inaccurate identifications. For example, we suspect the automated approach used by Mecozzi et al. (2016) to identify plastic fragments from a sea turtle gastrointestinal tract resulted in inaccurate results. Three fragments were identified as polyethylene oxide, which is typically a liquid at environmental temperatures. Manual assessment of the spectra may have avoided this potential mistake.

We validated the ability to differentiate HDPE and LDPE via the relative intensity of a small absorption band at 1377 cm^{-1}, which represents the more abundant methyl group in highly branched LDPE (Asensio et al., 2009; Nishikida & Coates, 2003; Brandon et al., 2016). For samples determined to be PE, the spectral region of 1400 cm^{-1} to 1330 cm^{-1} was examined closely by magnifying this region in Microsoft Excel scatterplots. PE spectra were binned into the following seven categories in which 1377 cm^{-1} was 1) absent, 2) a shoulder on 1368 cm^{-1}, 3) a small bump on 1368 cm^{-1}, 4) the second largest band in this region, 5) nearly equal to 1368 cm^{-1}, 6) the strongest band in this region, 7) detected as a band by the instrument's software. The confidence of each bin to identify the PE type was assessed in three ways. Firstly, the ATR FT-IR spectral bin was recorded for each SRM, scientifically sourced or raw manufactured plastic standards of known PE. Secondly, the densities of PE standards and debris samples categorized across the bins were estimated via a float/sink test in different dilutions of ethanol (200 proof, A.C.S. reagent grade, Acros Organics, Fair Lawn, NJ) in deionized water. Dilutions were prepared volumetrically with graduated cylinders and ranged from

238 23 % to 42 % ethanol with approximately 2 % increments. Density of the solutions was
239 measured by weighing 25 mL in a 25-mL graduated cylinder to the closest 0.0001 g.
240 Relative standard uncertainty in measuring the density of these solutions was 0.34 %.
241 The measured densities of all PE standards and 49 PE marine debris pieces collected
242 from Main Hawaiian Island beaches were used to assign the piece to either HDPE or
243 LDPE based on known densities of these polymers (Peacock, 2000; Verleye et al., 2001).
244 The percentage of HDPE or LDPE assignments via the float test within each bin provided
245 quantified confidence in using each bin and allowed us to set clear criteria. Thirdly,
246 tentative ATR FT-IR assignments of ingested plastics from sea turtles (samples described
247 below; 5 HDPE and 5 LDPE) were confirmed with HT-SEC with differential refractive
248 index, infrared, and multi-angle light scattering detection at NIST (methods described
249 below).
250 Differentiation between LLDPE and LDPE was tested by examining the regions
251 between 650 cm^{-1} and 1000 cm^{-1}. According to Nishikida & Coates (2003), absorbance
252 bands at 890 cm^{-1} (vinylidene group) and 910 cm^{-1} (terminal vinyl group) should be of
253 similar intensities and both weak for LLDPE, whereas they state that 890 cm^{-1} should be
254 predominant in LDPE. These spectra regions from one scientifically sourced LLDPE and
255 three consumer goods made of LLDPE were compared to several LDPE materials.
256
257 *2.3. Ingested Plastic Collection*
258
259 As described in Clukey et al. (2017), 2,880 ingested plastic pieces were found in
260 the gastrointestinal (GI) tracts of olive ridley (n = 37), green (n = 9), and loggerhead (n =
261 4) sea turtles caught incidentally by the Hawaiian and American Samoan longline fishery
262 between 2012 and 2015. Pieces were removed with hexane-rinsed forceps, rinsed with

nanopore deionized water, gently cleaned with cleanroom wipers, wrapped in hexane-rinsed foil, placed in a FEP bag, and archived frozen as part of the Biological and Environmental Monitoring and Archival of Sea Turtle tissues (BEMAST) project of the NIST Marine Environmental Specimen Bank (Keller et al., 2014).

2.4. Plastic Preparation

To minimize instrument time, a subset of pieces (n = 828) was selected for this study that visually represented all other pieces found in each turtle. A three-category rugosity scoring system was applied to some of the pieces and defined as (1) smooth, (2) ridged, and (3) rugose (Figure S1). Pieces were weighed before and after FT-IR analysis, repackaged and frozen for continued archival storage by BEMAST and future chemical analysis.

Eleven plastic fragments ingested by olive ridley sea turtles were chosen for testing five different cleaning methods, after being identified using absorption bands in Table 1 as HDPE (n = 3), LDPE (n = 5), and PP (n = 3). These fragments were analyzed by ATR FT-IR after undergoing five different treatments: (1) no additional cleaning, (2) wiping a small area with a dry cleanroom wiper, (3) wiping a new area with a cleanroom wiper that was wet with 70 % 2-propanol from a LDPE squirt bottle, (4) wiping a third area with a cleanroom wiper wet with deionized water from a LDPE squirt bottle, and (5) cutting the piece with hexane-rinsed scissors or pliers to expose the inside surface of the fragment. Three spectra were generated for each cleaning method on each piece by analyzing the fragment on three non-overlapping sections of the cleaned area. The optimal cleaning method was determined as described below in statistical methods. These less destructive cleaning methods were chosen over chemical manipulation with acids

288 and strong solvents as in Mecozzi et al. (2016) for green chemistry reasons and to
289 minimize manipulation so that the samples could be archived by BEMAST and tested in
290 the future for persistent organic pollutants.
291
292 *2.5. Analysis of ingested plastics for polymer type*
293
294 The 828 ingested plastic pieces discovered in the turtles were analyzed by ATR
295 FT-IR by first cleaning a small area with water and cleanroom wiper or cutting to expose
296 a smooth clean surface. Polymers were identified based on presence of absorption bands
297 as described in Table 1 and shown in Figure 1. Pieces producing absorption bands
298 consistent with both PE and PP were assigned as "mixture" (Figure 2). Pieces that could
299 not be identified by ATR FT-IR spectra (e.g., presence of less than four identifying
300 absorption bands) were assigned "unknown." A subset of pieces that were identified by
301 ATR FT-IR was analyzed by high HT-SEC with differential refractive index, infrared,
302 and multi-angle light scattering detection.
303 Samples for HT-SEC were sonicated in ethanol for 10 min, followed by 10 min
304 sonication in nanopure deionized water (18.2 MΩ) to remove aqueous soluble
305 contaminants and minimize the addition of biological contaminants to the instrument.
306 Approximately 10 mg of each sample was encased in a 5 µm stainless steel mesh and
307 dissolved in HPLC grade 1,2,4-trichlorobenzene under nitrogen atmosphere for 1 h prior
308 to injection in the instrument, allowing soluble polymers to dissolve and pass through the
309 mesh, and insoluble debris, filler, or crosslinked components to remain sequestered in the
310 mesh. The samples were injected into a Polymer Characterization (Valencia, Spain)
311 GPC-IR instrument with an IR 4 detector consisting of two infrared IR detection bands,
312 2800 cm^{-1} to 3000 cm^{-1} representing the entire C-H stretching region (CH, CH_2, and

313 CH_3), and a narrow band at 2950 cm^{-1} for the methyl C-H stretch absorbances,
314 respectively, as well as a Wyatt Technology (Santa Barbara, CA) Dawn Heleos II multi-
315 angle light scattering (MALS) detector with 18 angles and a forward monitor (zero angle
316 detector). Separately, the samples were also injected on a Tosoh (Tokyo, Japan) HT-Eco
317 SEC with differential refractive index detection. Both instruments ran at 160 °C with a
318 1,2,4-trichlorobenzene mobile phase with 300 ppm Irganox 1010 added as an antioxidant.
319 The stationary phase columns used in both systems are a set of three Tosoh HT2 columns
320 (two, Tosoh TSKgel GMHhr-H (S) HT2, 13 µm mixed bed, 7.8 mm ID × 30 cm columns
321 and one, Tosoh TSKgel GMHHR-H (20) HT2, 20 µm, 7.8 mm ID × 30 cm column with
322 an exclusion limit ≈ 4 x 10^8 g/mol). Sample molar masses, molar mass distribution, short
323 chain branching content (SCB), were determined by calibration with narrow molar mass
324 distribution PS standards, NIST SRM 1475a (linear, broad, HDPE), and NIST SRM 1478
325 (to determine inter-detector delay and normalize photodiode response of the MALS
326 detector), and 10 blends of linear PE and PP with systematic variation of PP content,
327 where the total degree of short chain branching (SCB) was confirmed by nuclear
328 magnetic resonance spectroscopy (NMR). Calibration and data analysis was performed
329 by proprietary software from each instrument vendor. HT-SEC and NMR have many
330 advantages, but they can only measure polymer chains that are soluble under the solvent
331 and temperature conditions used and they are not high-throughput like ATR-FTIR, which
332 measures the bulk sample.

333
334 2.6. *Data handling and statistical analysis*
335
336 Ordination was used to synthesize the absorbance data, in order to: 1) determine if
337 novel absorption bands at additional wavenumbers could distinguish HDPE and LDPE,

and 2) investigate if clustering of "unknown" ingested pieces near known polymers could help to identify their polymer composition. MetaboAnalyst software was used and the "normalized by sum" option was chosen so that all spectral bands had equal weight and samples could be compared. Two principal component analyses (PCAs) were performed on different sample sets. PCA1 included spectra from three consumer goods of each of the following polymers: HDPE, LDPE, and PP. PCA2 included 797 ingested plastic pieces (793 identified, 4 unknown) of nine identified polymer types. Because PCA requires at least three samples of each polymer and less than three ingested pieces of PVC and nylon were discovered, it was necessary to include the spectra of consumer good items representing PVC and nylon in PCA2. PCA1 was run using bins of four wavenumbers over the entire spectral range of 4000 cm^{-1} to 450 cm^{-1} while PCA2 used selected absorption bands within a range of ± 1 cm^{-1} identified in Table 1 (plus additional bands from the literature) for polymers included in the analysis. All possible absorption bands were included in PCA1 to discover novel absorption bands for distinguishing HDPE from LDPE. No transformations were performed and Pareto scaling was used for both PCAs.

The optimal cleaning method was determined in two ways: 1) determining the percent of spectra that provided visually identifiable polymer assignment (good vs. poor quality spectra), and 2) counting the number of detectable absorption bands used for identification of that particular polymer. Wavenumbers with absorption bands greater than three times the noise surrounding the absorption band were recorded as detectable wavenumbers. All variables were tested for normality using the Shapiro-Wilk tests in IBM SPSS Statistics Version 24. Because normality could not be accomplished even

after data transformations, non-parametric Friedman's ANOVA tests followed by Wilcoxon signed-rank tests were used to compare differences in cleaning methods using two different response variables: percent of identifiable spectra and number of identifiable absorption bands greater than three times the noise. A Spearman Rank Order correlation was used to determine if rugosity had an effect on the number of detectable wavenumbers.

3. Results and Discussion

3.1. ATR FT-IR polymer identification of consumer goods, raw manufactured, or scientifically sourced polymers

Plastic consumer goods from known resin codes produced spectra with expected absorption bands (Figure 1, Table 1). When compared to the spectra of raw manufactured polymers or scientifically sourced polymers, the appearance and number of identifiable wavenumbers were nearly identical (data not shown). Absorption bands identified for these polymers were either a direct match or within four wavenumbers of the absorption bands listed in Table 1. Of the 18 polymers tested, all could be easily distinguished from each other with only three minor exceptions (Figure 1). Spectra of FEP and PTFE showed absorbance bands at the same wavenumbers and with the same intensity for 638 cm^{-1}, 554 cm^{-1}, and 509 cm^{-1}, but the intensity of 1201 cm^{-1} (CF_2 stretch) and 1147 cm^{-1} (CF_2 stretch) were 16 % and 27 % higher, respectively, in PTFE than FEP. All types of nylon produced the same absorbance bands, so nylon-12 cannot be distinguished from nylon 6,6 or others (Verleye et al., 2001). Differentiating among HDPE, LLDPE, and LDPE is challenging, but our goal was to develop a simple ATR FT-IR method so that discrimination by sample destructive methods, such as HT-SEC with infrared detection or

387 differential scanning calorimetry (DSC), is not required. Our results confirm that ATR
388 FT-IR can identify consumer goods produced from PETE, PEs, PVC, PP, PS, ABS, CA,
389 EVA, latex, nitrile, nylons, PC, PMMA, (PTFE or FEP), and PU, but PE samples require
390 closer inspection of the ATR FT-IR spectra to distinguish HDPE from LDPE.

391 The use of ATR FT-IR for polymer identification was further confirmed via a
392 blind test, in which 11 consumer goods consisting of diverse polymers were correctly
393 identified by an analyst without prior knowledge of the resin code (Table S1). The five
394 PE samples were all correctly identified as PE, but some could not be further categorized
395 as either HDPE or LDPE. Of the three HDPE samples, one was correctly assigned and
396 two were categorized as unknown PE. Of the two LDPE, one was correctly assigned and
397 one was assigned unknown PE.

398 In hopes of discovering additional absorbance bands to distinguish HDPE from
399 LDPE, a PCA was performed including the spectra of consumer goods of HDPE (n = 3),
400 LDPE (n = 3), and PP (n = 3). The PCA showed no separation between HDPE and LDPE
401 (Figure S2). The first two principal components (PC) explained 78.3 % of the variance
402 and the loadings are shown in Table S2. This biplot revealed absorbance bands that
403 differentiate PE from PP (700 cm^{-1} to 730 cm^{-1}, CH_2 rock), but no novel bands that could
404 distinguish HDPE from LDPE (Figure S2). While additional PCs explained more of the
405 variation (14.7 % by PC3 and 6 % by PC4), they did not provide any additional
406 separation of HDPE from LDPE. This is because HDPE and LDPE share the same major
407 structural unit, functional groups, chemical bonds (Asensio et al., 2009), and therefore
408 have many identical wavenumbers (Table 1). However, the different degree of branching
409 results in small, but important differences, in the spectral region of 1400 cm^{-1} to 1330 cm^{-}

410 [1] with LDPE having greater intensity at 1377 cm^{-1} due to methyl bending deformation of
411 the branched chain ends (Asensio et al., 2009; Nishikida & Coates, 2003). This band may
412 have been too small for the PCA to detect and must be magnified and compared to the
413 intensity of 1368 cm^{-1} manually.
414 The differentiation between LDPE and HDPE with the presence of a 1377 cm^{-1}
415 band is easy in some spectra, while others are more challenging. PE spectra fell into
416 seven different bins based on the observation of the 1377 cm^{-1} band being: 1.) absent, 2.)
417 a tiny shoulder, 3.) a small bump, 4.) the second largest in the 1400 cm^{-1} to 1330 cm^{-1}
418 region, 5.) nearly equivalent to 1368 cm^{-1} band, 6.) the largest in this region, and 7.)
419 detected by the instrument's software (Figure 3). Bins at the extremes (1 and 2 are
420 HDPE; 6 and 7 are LDPE) are clear, but those in the middle are ambiguous (bins 3, 4,
421 and 5) and cause substantial confusion.
422 Table S1 describes ATR FT-IR results of each standard and consumer good
423 tested. All but one of the SRMs, raw manufactured plastic or scientifically sourced
424 standards of known PE (n=10 for HDPE, n=4 LLDPE, and n=17 LDPE) were correctly
425 and easily assigned because they fell in the clear bins (Table S1). One LDPE standard,
426 SRM 1474b, fell into bin 3. Fourteen consumer good standards were stamped with HDPE
427 (n=6), LLDPE (n=3), or LDPE (n=5). Of these, eight (57 %) were accurately assigned
428 because they produced unambiguous spectra, six (43 %) produced ambiguous spectra,
429 and one (0.1 %) with a clear spectrum was inaccurately assigned. Three of the six
430 ambiguous samples were thin bags used for produce, shopping, and shipping. The
431 incorrect standard was a grocery shopping bag stamped with #2 resin code (HDPE), but
432 1377 cm^{-1} was the strongest peak. These results suggest that thin sheet bags are

consistently the most ambiguous and challenging to assign to HDPE versus LDPE for reasons currently unknown.

The other three ambiguous spectra came from all three LLDPE consumer goods tested. Because LLDPE has intermediate extents of branching, this was not surprising. Unfortunately, bins 3, 4, and 5 cannot be considered LLDPE, because materials known to be HDPE and LDPE also produced spectra in these bins. A method to distinguish LLDPE from LDPE samples was proposed using another region of the spectra (650 cm^{-1} to 1000 cm^{-1}) by Nishikida & Coates (2003). They report that LLDPE should have equal and weak bands at 890 cm^{-1} (vinylidene group) and 910 cm^{-1} (terminal vinyl group), whereas 890 cm^{-1} is larger in LDPE. We could not confirm this method with a close examination of this spectral region with four LLDPE and 18 LDPE standards (Table S1). The four known LLDPE standards produced variable results. The LLDPE trash bag had equally weak bands, as expected. The LLDPE biohazard bag produced a band at 890 cm^{-1} was larger but nearly equal to the 910 cm^{-1} band. However, the scientifically sourced LLDPE sample produced no band at 890 cm^{-1} and a small band at 910 cm^{-1}, and the LLDPE tubing produced a larger band at 910 cm^{-1} than 890 cm^{-1}. As expected, 14 of the 18 LDPE samples (78 %) produced a more intense 890 cm^{-1} band than 910 cm^{-1}. Three materials produced equally intense peaks (SRM 1476a, a swimmer's ear bottle, and a shipping bag), and for this reason we suspect they were produced with LLDPE. One produced a very small band at 910 cm^{-1} and no band at 890 cm^{-1} (a breastmilk storage bag). The inconsistent results within the known LLDPE standards did not give enough confidence to use this distinguishing method. Therefore, we conclude that LLDPE and LDPE cannot be distinguished from each other using ATR FT-IR.

456 In the ambiguous bins 3, 4, and 5, the 1377 cm^{-1} band appears as a small bump on
457 the tail of the 1368 cm^{-1} band, a distinct but smaller band than 1368 cm^{-1}, or equivalent to
458 the intensity of 1368 cm^{-1}, respectively. Confidence to assign these bins to a particular PE
459 was assessed, for the first time to our knowledge, by estimating the density of PE samples
460 using a float/sink test in different dilutions of ethanol. Using a graduated cylinder to
461 volumetrically prepare solutions resulted in inaccuracies of solution densities of up to
462 0.02 g/mL. Because distinguishing between 0.93 g/mL and 0.94 g/mL required better
463 accuracy, the density of the solutions was determined by weighing 25 mL in a graduated
464 cylinder. Relative standard uncertainty in measuring the density of these solutions
465 was 0.34 %. Resulting estimated densities for each standard item are shown in Table S1.
466 All PE standards that were not stamped or labeled with a resin code that were
467 subsequently assigned LDPE because they fell in bins 6 and 7 (n=4), floated in solutions
468 greater than 0.931 g/mL as expected. This added more confidence to our LDPE criteria.
469 Furthermore, 19 of the 20 known LDPE or LLDPE standards (95 %) tested had estimated
470 densities of 0.938 g/mL or less; and all ten known HDPE standards had estimated
471 densities of 0.938 g/mL or greater. Unexpectedly, one LDPE thin shipping bag sank in
472 solutions up to 0.950 g/mL. Its greater density may be attributed to a silver-colored inner
473 layer of unknown polymer composition.
474 Because our methods to differentiate HDPE from LDPE were slightly less
475 successful in consumer goods than in raw or scientifically sourced standards, we
476 confirmed our method using marine debris samples. Forty-nine plastic debris items
477 collected from Main Hawaiian Island beaches that were discovered to be PE by ATR FT-
478 IR were categorized as bin 1 (n=3), bin 2 (n=14), bin 3 (n=1), bin 4 (n=5), bin 5 (n=13),

and bin 6 (n=13). These fragments were tested for floating or sinking in solutions with targeted densities of 0.935 g/mL and 0.941 g/mL. All of bin 1 samples sank, as expected for HDPE. 86 % of bin 2 samples sank, providing enough confidence to conclude spectra with a shoulder at 1377 cm^{-1} are very likely HDPE. The one sample in bin 3 sank, suggesting samples producing a very small bump at 1377 cm^{-1} are HDPE, but our sample size was too small to have certainty. Only 40 % of bin 4 and 46 % of bin 5 floated in both solutions, suggesting these polymers could be either HDPE or LDPE when 1377 cm^{-1} is the second largest band or equivalent to 1368 cm^{-1}. 85 % of bin 6 samples floated in both solutions, giving us enough confidence to confirm that spectra with 1377 cm^{-1} as the largest band are likely LDPE, even though the instrument's software does not detect it.

The inter-laboratory comparison using HT-SEC on PE ingested plastic samples, confirmed that ATR FT-IR assignments were 100 % accurate (Table 3). These samples all produced unambiguous spectra (n=5 HDPE, n=5 LDPE). Taken together the results suggest there is a high confidence in unambiguous ATR FT-IR spectra to distinguish HDPE from LDPE. However, ambiguous spectra (bins 3-5) cannot be assigned to a particular PE polymer without further testing, and ATR FT-IR spectra cannot be used to distinguish LDPE from LLDPE. A detailed step-by-step decision tree outlines our criteria for distinguishing HDPE from LDPE using ATR FT-IR in addition to a float/sink test (Figure 3). Once samples are determined to be PE based on absorbance bands listed in Table 1, the spectral region between 1330 cm^{-1} and 1400 cm^{-1} is magnified and each sample is matched to the most similar bin. Samples falling in bins 1 and 2 are assigned HDPE. Those in bins 3-5 are considered unknown PE until further testing can be done. Those in bins 6 and 7 are assigned LDPE or LLDPE. The unknown PE samples that are

not air-filled can be placed into a 0.935 g/mL solution of ethanol. If they float, they are assigned LDPE or LLDPE. If they sink, they are assigned HDPE. The approach described in this decision tree should help future studies with the often confusing, yet very important, differentiation of HDPE and LDPE.

3.2. Cleaning methods for polymer identification of ingested plastics

To our knowledge, no study had addressed how digestive processes affect the FT-IR spectra of polymers, so we determined an optimal cleaning method that would also preserve the samples for future chemical testing. The spectra from the 11 ingested fragments after cleaning with water were of higher quality and easier to identify than before cleaning (Figure S3), with the noise reduced and the absorbance bands more prominent. Thus, this test suggests that this simple treatment, involving removing surface residue with a cleanroom wiper and water, increases the ability to identify plastic polymers.

Only half of the spectra were of good enough quality to identify the polymer when no cleaning was performed on the samples (58 % ± 29 % standard deviation), whereas 100 % of spectra were identifiable with the other four cleaning methods (Figure S4). Significant differences in the percent of spectra that could be identified were found among the five cleaning methods (Friedman's analysis of variance (ANOVA), $x^2(4) = 26.20$, $p < 0.0001$, $n = 11$). Post-hoc comparisons using Wilcoxon signed-rank tests revealed that all four sample treatments (wiping ($p = 0.004$, $n = 11$), cleaning with 2-propanol ($p = 0.004$, $n = 11$), water ($p = 0.004$, $n = 11$), or cutting ($p = 0.004$, $n = 11$)) resulted in a greater percentage of the spectra being identified, when compared to no cleaning (Figure S4). No significant differences were found among the four cleaning

527 methods. These results suggest that cleaning a polymer of ingested plastic fragments with
528 any of the four methods should improve quality of ATR FT-IR spectra.
529 The number of detected peaks increased significantly for all three polymer types
530 after performing any of the four cleaning methods (Figure 4). The number of detected
531 peaks and rugosity codes for each cleaning method for each fragment can be found in
532 Table S3. Significant differences were found among the five cleaning methods for HDPE
533 (Friedman's ANOVAs, $x^2(4) = 27.41$, $p < 0.0001$), for LDPE ($x^2(4) = 34.992$, $p < 0.0001$)
534 and for PP ($x^2(4) = 19.92$, $p = 0.001$). For HPDE, wiping (Wilcoxon $p = 0.007$), 2-
535 propanol ($p = 0.006$), water ($p = 0.005$), and cutting ($p = 0.018$) produced significantly
536 more detectable peaks than no treatment. Cleaning HDPE fragments with water also
537 produced significantly more detectable peaks when compared to wiping ($p = 0.008$), 2-
538 propanol ($p = 0.008$), and cutting ($p = 0.014$). Similar results were seen with PP and
539 LDPE ingested fragments (Figure 4). These differences suggest that cleaning the surface
540 of ingested fragments with water will produce the spectrum with the most detectable
541 peaks and this method might be preferred if the goal is to minimize handling so that the
542 pieces can be used in the future for additional chemical testing, such as measuring sorbed
543 persistent organic pollutants.
544
545 LDPE fragments with a higher rugosity code yielded fewer detectable peaks ($r_s =$
546 -0.803, $n = 5$, $p = 0.102$), although the relationship was not significant (Figure S5). In
547 contrast, when fragments were cut, no significant correlation was found between the
548 number of detectable peaks and rugosity codes ($r_s = 0.631$, $n = 5$, $p = 0.254$). This is most
549 likely due to rugosity being reduced when a fragment is cut. Therefore, if a rugose
550 fragment cannot be identified after being cleaned with water, cutting may be the most

551 effective cleaning method as it can allow for the sample to come in more direct contact
552 with the diamond and thus evanescent wave, resulting in more detectable peaks.
553
554 *3.3. Method validation with ingested polymers*
555
556 Only 30 of the 828 ingested plastic pieces analyzed (4 %) produced spectra of
557 poor quality that could not be identified by ATR FT-IR. Criteria for differentiating HDPE
558 and LDPE (even without the float/sink test, which was not applied to these samples)
559 allowed assignment of 77.7 % of the PE pieces, while 22.3 % of PE samples fell in the
560 unknown PE category. This proportion is similar to the 70 % assignment capability of
561 oceanic microplastics by Brandon et al. (2016).
562 PCA was performed on spectra from 797 representative ingested plastic pieces
563 identified as HDPE (n = 58), PVC (n = 1), LDPE or LLDPE (n = 310; one outlier was
564 removed), PP (n = 270; one outlier was removed), PS (n = 7), nylon (n = 1), mixture of
565 PP and PE (n = 40), unknown PE (n = 106) and unknown (n = 4) along with plastic
566 consumer goods of PVC and nylon. The PCA shows distinction between PEs and PP
567 (Figure 5; Table S4 for loadings) with 85.8 % of the variance explained within the first
568 two principal components. In an earlier version of the PCA, more of the ingested pieces,
569 a total of 10, were originally identified as unknown (data not shown). The clustering of
570 six of the unknown samples within the PCA, followed by further review of their ATR
571 FT-IR spectra, allowed polymer assignment of these samples. These results suggest that
572 PCA is a tool that can help interpret ambiguous spectra. Plastic pieces identified as a
573 mixture were located between clusters for PE and PP as expected. In order to improve
574 assignment of these predominantly olefinic polymers, HT-SEC with multiple detectors

575 was used to definitively identify the samples as a mixture of PE and PP, and confirm
576 results of the PCA.
577 Sixteen of 17 ingested plastic samples were positively identified by HT-SEC. All
578 HT-SEC determined identities matched those obtained by ATR FT-IR, as shown in Table
579 3. Example chromatograms for three samples, identified as PS, LDPE, and HDPE are
580 shown in Figure 6. A number of qualitative and quantitative pieces of information were
581 used to identify the polymers analyzed by HT-SEC. First, the injected polymer samples
582 demonstrated a positive or negative differential refractive index (RI) peak as they eluted
583 from the columns, indicative that the polymer had a greater or lesser refractive index than
584 the mobile phase ($n_0 = 1.56$). Refractive indices of commercial polymers are available
585 from a number of sources (Brandrup et al., 1999, Mark, 2007). This qualitative
586 identification is used to rule out general classes of polymers; for example, polyolefins
587 (PP, HDPE, LDPE) have a refractive index less than 1.56, so these polymers must have a
588 negative RI elution peak (Table 3, Figure 6 b and c).
589 Differentiation between PP, HDPE, and LDPE was based on the degree of short
590 chain branching, which was measured using the HT-SEC IR detector. The flow-through
591 IR detector measures alkyl and methyl C-H stretching simultaneously as the separated
592 polymer elutes. The ratio of the two absorption spectra at each elution volume (Figure 6),
593 when compared to a calibration curve, permit branching content to be determined across
594 the molar mass distribution. As ATR FT-IR is a bulk measurement, the branching content
595 measured by HT-SEC was averaged across the molar mass distribution for each sample
596 and the average methyl content per 1000 total carbons (CH_3/1000 total C) is shown in
597 Table 3. HDPE is identified from samples that have 10 CH_3/1000 total C or less, as the

598 only CH_3 contributions in HDPE are from chain ends, which are negligible. This is also a
599 convenient metric as the limit of detection for the IR detector is 10 CH_3/1000 total C. PP
600 was identified for polymers with a methyl content of (330 ± 33) CH_3/1000 total C, which
601 is determined from theoretical calculations based on the propylene repeat unit. The 10 %
602 tolerance is to include PP that may have some small degrees of degradation from the
603 turtle digestive tract as well as account for small variations (< 10 %) that were observed
604 in HT-SEC analysis of consumer-grade PP (stamped resin code 5) when compared to
605 reagent grade PP obtained from Sigma Aldrich. Currently, there is no documentary
606 standard that specifies what purity a consumer polymer must have to be stamped with a
607 specific resin code. LDPE is assigned to polymers with an average branching content
608 between HDPE and PP, or (10 to 300) CH_3/1000 total C. For the purposes of this study,
609 no effort was made to distinguish LLDPE from LDPE in ingested plastics, as ATR FT-IR
610 cannot make that distinction. Future studies will address distinguishing LLDPE from
611 LDPE in unknown polymer samples and mixtures with the addition of a differential
612 viscometer to measure long chain branching.
613 Three of the 17 samples were identified as PS (Figure 6a) based on several lines
614 of evidence. Their positive differential RI signal and minimal alkyl content lead to small
615 IR peak areas and large standard deviations in CH_3/1000 total C determinations. Also,
616 there was agreement between polymer number average (M_n) and mass average (M_w)
617 molar masses determined by MALS (considered an absolute measurement technique) and
618 those determined by relative comparison to polystyrene standards. M_n and M_w values
619 were determined for all samples and are listed as information values in Table 3.

One sample measured by HT-SEC (assigned as PETE by ATR FT-IR) was completely insoluble in 1,2,4-trichlorobenzene at 160 °C, and no peaks were not observed in HT-SEC chromatograms using any detector. The second independent assignment of this sample was instead based on survey x-ray photoelectron spectroscopy (XPS) to measure the elemental composition in the sample. Elemental composition of this sample was (80.3 ± 0.9) % C, (3.6 ± 0.3) % N, and (15.0 ± 0.9) % O, plus additional trace elements (silica and calcium and sodium salts), taken as an average of three locations on the sample. A tentative assignment of PU was made on the material, as the carbon, nitrogen, and oxygen content was closest to database values for PU at 78.6 %, 8.4%, and 14 %, respectively. As XPS only excites photoelectrons within the first ≈10 nm of a material, further sampling and measurements of the material will have to be performed. While this piece of brown fabric produced an ATR FT-IR spectrum with six absorption bands matching PETE, it was a poor-quality spectrum. XPS database values for PETE are 68.9 % carbon, 31.1 % oxygen, and do not contain nitrogen, which are generally more different from the readings of this fabric piece than those of PU. Taking all data into account, this piece was assigned PU.

With the exception of one misidentification, these novel inter-laboratory results support using ATR FT-IR to identify polymers of degraded and ingested plastics. Identifying the polymers comprising ingested plastic using this simple, accurate method can help us understand many aspects of the marine debris problem. The polymer type will dictate the transport and fate of marine debris and its affinity for other chemical pollutants. Furthermore, knowing the predominant polymer can inform better conservation and management practices. For example, LDPE and PP (resin code #4 and

643 #5) represent large proportions of marine debris and are not commonly recycled in the
644 Hawaiian Islands. Incentive programs for recycling these polymers and innovative post-
645 use applications could be prioritized to help reduce the abundance of LDPE and PP in the
646 marine environment.
647
648 **4. Conclusion**
649
650 As the ingestion of plastic debris by threatened marine species such as sea turtles
651 increases, the need to categorize plastic debris by polymer type and identify marine
652 transport mechanisms and fates has become a high research priority. Here, we provide a
653 definitive validation of ATR FT-IR to identify ingested plastic polymer types, including
654 resin codes #1 through #6 and many polymers within code #7 without the use of a costly
655 database. A clear, easy to follow guide of thoroughly tested criteria was presented to
656 confidently differentiate HDPE and LDPE. Our approach has been successfully used by
657 four additional ongoing marine debris studies with macro to microplastics found in water,
658 on beaches, or ingested by other marine organisms. We encourage future studies to
659 prepare ingested plastic samples by cleaning them with water or cutting rugose pieces to
660 get a clean surface prior to ATR FT-IR analysis to produce the most accurate results.
661 PCA can be leveraged to assign polymer types to the small proportion of pieces that
662 present challenging ATR FT-IR spectra. This method has been used to identify the
663 polymer composition ingested by three species of sea turtles in the pelagic Pacific.
664 Results on polymers ingested by sea turtle species, geographical, and other comparisons
665 will be reported in a forthcoming manuscript (Jung, in preparation). The data reported in
666 the current method development study represent only selected pieces; therefore,

667 calculating the percentage of each polymer reported here would misrepresent the actual
668 ingested composition.
669 The accuracy of using ATR FT-IR for identifying commercial polymers in marine
670 debris, as demonstrated in this study, has the benefit of rapid analysis and minimal
671 destruction to the collected samples, which is ideal for high throughput analysis of large
672 repositories of marine debris. There is, however, much more detailed information about
673 discarded plastics that can be explored by utilizing advanced polymer metrology
674 methods, such as HT-SEC, thermal analysis, or rheological measurements. Systematic
675 changes in chemical composition, molar mass, molar mass distribution and viscoelastic
676 properties in a specific polymeric resin can provide better understanding of material
677 degradation pathways and resulting byproducts. Comprehensive understanding of the
678 origins, transport, fate, and lifetime of marine debris will ultimately require both high-
679 throughput and fundamental studies of discarded materials, providing ample
680 opportunities for collaboration between the life sciences and material science
681 communities to address the challenges in marine plastics moving forward.
682
683 **Disclaimer**
684
685 Certain commercial equipment, instruments, or materials are identified in this paper to
686 specify adequately the experimental procedure. Such identification does not imply
687 recommendation or endorsement by the National Institute of Standards and Technology,
688 nor does it imply that the materials or equipment identified are necessarily the best
689 available for the purpose.
690
691 **Acknowledgements**
692

693 Funding was provided by grant 60NANB15D026 from the U.S. Pacific Islands
694 Program of the NIST Marine Environmental Specimen Bank. The ATR FT-IR instrument
695 was supported by National Institutes of Health grant P20GM103466. We thank Stacy
696 (Vander Pol) Schuur for providing some of the raw manufactured polymers. We thank
697 Tracy Schock for her advice on principal component analyses. We thank the fishermen
698 and fisheries observers for carefully assessing, storing, and transporting the sea turtle
699 specimens. We thank Shandell Brunson, Irene Nurzia Humburg, Devon Franke, Emily
700 Walker, Sarah Alessi, T. Todd Jones (PIFSC), Bob Rameyer (USGS), Katherine Clukey,
701 Jessica Jacob, Frannie Nilsen, Julia Smith, Adam Kurtz, Angela Hansen, Stephanie
702 Shaw, Jennette VanderJagt, and Jessica Kent (Hawaii Pacific University) and numerous
703 other volunteers for help in sample collection and processing. We thank the entire NIST
704 Marine Environmental Specimen Bank team, especially Rebecca Pugh and Paul Becker,
705 for sample archival. Finally, we thank Chris Stafford, Amanda Forster and Rebecca Pugh
706 for comments on the draft manuscript. Mention of products and trade names does not
707 imply endorsement by the U.S. Government.
708

709 **Appendix A. Supplementary data**

710 Supplementary data to this article can be found online at XXX.
711

712 Literature Cited
713

714 Andrady, A.L., 2017. The plastic in microplastics: A review. *Marine Pollution Bulletin*,
715 *119*(1), pp.12-22.
716 Andrady, A.L., 2011. Microplastics in the marine environment. *Marine Pollution*
717 *Bulletin*, *62*(8), pp.1596-1605.
718 Asefnejad, A., Khorasani, M.T., Behnamghader, A., Farsadzadeh, B. and Bonakdar, S.,
719 2011. Manufacturing of biodegradable polyurethane scaffolds based on
720 polycaprolactone using a phase separation method: physical properties and in
721 vitro assay. *International Journal of Nanomedicine*, *6*, p.2375.
722 Asensio, R.C., Moya, M.S.A., de la Roja, J.M. and Gómez, M., 2009. Analytical
723 characterization of polymers used in conservation and restoration by ATR-FTIR
724 spectroscopy. *Analytical and Bioanalytical Chemistry*, *395*(7), pp.2081-2096.
725 ASTM International. 2013. Standard Practice for Coding Plastic Manufactured Articles
726 for Resin Identification. Designation: D7611/D7611M – $13^{\varepsilon 1}$.
727 Bakir, A., Rowland, S.J. and Thompson, R.C., 2014. Enhanced desorption of persistent
728 organic pollutants from microplastics under simulated physiological conditions.
729 *Environmental Pollution*, *185*, pp.16-23.
730 Beltran, M. and Marcilla, A., 1997. Fourier transform infrared spectroscopy applied to
731 the study of PVC decomposition. *European Polymer Journal*, *33*(7), pp.1135-
732 1142.
733 Bjorndal, K.A., Bolten, A.B. and Lagueux, C.J., 1994. Ingestion of marine debris by
734 juvenile sea turtles in coastal Florida habitats. *Marine Pollution Bulletin*, *28*(3),
735 pp.154-158.
736 Brandon, J., Goldstein, M. and Ohman, M.D., 2016. Long-term aging and degradation of
737 microplastic particles: Comparing in situ oceanic and experimental weathering
738 patterns. *Marine Pollution Bulletin*, *110*(1), pp.299-308.
739 Brandrup, J., Immergut, E.H. and Grulke, E.A., 1999. *Polymer Handbook (Fourth*
740 *Edition)*. New York: John Wiley & Sons, Inc., pp.2336.
741 Bugoni, L., Krause, L. and Petry, M.V., 2001. Marine debris and human impacts on sea
742 turtles in southern Brazil. *Marine Pollution Bulletin*, *42*(12), pp.1330-1334.
743 Cincinelli, A., Scopetani, C., Chelazzi, D., Lombardini, E., Martellini, T., Katsoyiannis,
744 A., Fossi, M.C. and Corsolini, S., 2017. Microplastic in the surface waters of the
745 Ross Sea (Antarctica): Occurrence, distribution and characterization by FTIR.
746 *Chemosphere*, *175*, pp.391-400.
747 Clukey, K.E., Lepczyk, C.A., Balazs, G.H., Work, T.M. and Lynch, J.M., 2017.
748 Investigation of plastic debris ingestion by four species of sea turtles
749 collected as bycatch in pelagic Pacific longline fisheries. *Marine Pollution*
750 *Bulletin*, 120(1-2), pg.117-125.
751 Coates, J., 2000. Interpretation of infrared spectra, a practical approach. In: Meyers, R.A.
752 (editor) *Encyclopedia of Analytical Chemistry*. Chichester: John Wiley & Sons,
753 Ltd., pp.10815-10837.
754 Cole, M. and Galloway, T.S., 2015. Ingestion of nanoplastics and microplastics by
755 Pacific oyster larvae, *Environmental Science & Technology*, *49*(24), pp.14625-
756 14632.

Cole, M., Webb, H., Lindeque, P.K., Fileman, E.S., Halsband, C. and Galloway, T.S., 2014. Isolation of microplastics in biota-rich seawater samples and marine organisms. *Scientific Reports*, *4*, p.4528.

Dümichen, E., Barthel, A.K., Braun, U., Bannick, C.G., Brand, K., Jekel, M. and Senz, R., 2015. Analysis of polyethylene microplastics in environmental samples, using a thermal decomposition method. *Water Research*, *85*, pp.451-457.

Endo, S., Takizawa, R., Okuda, K., Takada, H., Chiba, K., Kanehiro, H., Ogi, H., Yamashita, R. and Date, T., 2005. Concentration of polychlorinated biphenyls (PCBs) in beached resin pellets: variability among individual particles and regional differences. *Marine Pollution Bulletin*, *50*(10), pp.1103-1114.

Fischer, M. and Scholz-Böttcher, B.M., 2017. Simultaneous trace identification and quantification of common types of microplastics in environmental samples by pyrolysis-gas chromatography-mass spectrometry. *Environmental Science & Technology*, *51*(9), p.5052.

Frère, L., Paul-Pont, I., Moreau, J., Soudant, P., Lambert, C., Huvet, A. and Rinnert, E., 2016. A semi-automated Raman micro-spectroscopy method for morphological and chemical characterizations of microplastic litter. *Marine Pollution Bulletin*, *113*(1), pp.461-468.

Fries, E. and Zarfl, C., 2012. Sorption of polycyclic aromatic hydrocarbons (PAHs) to low and high density polyethylene (PE). *Environmental Science and Pollution Research*, *19*(4), pp.1296-1304.

Geyer, R., Jambeck, J.R. and Law, K.L., 2017. Production, use, and fate of all plastics ever made. *Science Advances*, *3*(7), p.e1700782.

Guidelli, E.J., Ramos, A.P., Zaniquelli, M.E.D. and Baffa, O., 2011. Green synthesis of colloidal silver nanoparticles using natural rubber latex extracted from Hevea brasiliensis. *Spectrochimica Acta Part A: Molecular and Biomolecular Spectroscopy*, *82*(1), pp.140-145.

Hoarau, L., Ainley, L., Jean, C. and Ciccione, S., 2014. Ingestion and defecation of marine debris by loggerhead sea turtles, Caretta caretta, from by-catches in the South-West Indian Ocean. *Marine Pollution Bulletin*, *84*(1), pp.90-96.

Hoss, D.E. and Settle, L.R., 1990. Ingestion of plastics by teleost fishes. In *Proceedings of the Second International Conference on Marine Debris. NOAA Technical Memorandum. NOAA-TM-NMFS-SWFSC-154. Miami, FL*, pp.693-709.

Howell, E.A., Bograd, S.J., Morishige, C., Seki, M.P. and Polovina, J.J., 2012. On North Pacific circulation and associated marine debris concentration. *Marine Pollution Bulletin*, *65*(1), pp.16-22.

Ilharco, L.M. and Brito de Barros, R., 2000. Aggregation of pseudoisocyanine iodide in cellulose acetate films: structural characterization by FTIR. *Langmuir*, *16*(24), pp.9331-9337.

Jambeck, J.R., Geyer, R., Wilcox, C., Siegler, T.R., Perryman, M., Andrady, A., Narayan, R. and Law, K.L., 2015. Plastic waste inputs from land into the ocean. *Science*, *347*(6223), pp.768-771.

Jung, M. in preparation. Polymer Identification of Plastic Debris Ingested by Pelagic-phase Sea Turtles in the Central Pacific. Master Thesis. Hawaii Pacific University, Kaneohe, HI.

802 Koelmans, A.A., Besseling, E., Wegner, A. and Foekema, E.M., 2013. Plastic as a carrier
803 of POPs to aquatic organisms: a model analysis. *Environmental Science &*
804 *Technology*, *47*(14), pp.7812-7820.
805 Keller, J.M., Pugh, R.S. and Becker, P.R., 2014. Biological and Environmental
806 monitoring and archive of sea turtle tissues (BEMAST): Rationale, protocols, and
807 initial collections of banked sea turtle tissues. *NIST Internal Report (NISTIR)-*
808 *7996*.
809 Mark, J.E. ed., 2007. *Physical Properties of Polymers Handbook* (Vol. 1076). New York:
810 Springer.
811 McIlgorm, A., Campbell, H.F. and Rule, M.J., 2011. The economic cost and control of
812 marine debris damage in the Asia-Pacific region. *Ocean & Coastal Management*,
813 *54*(9), pp.643-651.
814 Mecozzi, M., Pietroletti, M. and Monakhova, Y.B., 2016. FTIR spectroscopy supported
815 by statistical techniques for the structural characterization of plastic debris in the
816 marine environment: Application to monitoring studies. *Marine Pollution*
817 *Bulletin*, *106*(1), pp.155-161.
818 Moore, C.J., Moore, S.L., Leecaster, M.K. and Weisberg, S.B., 2001. A comparison of
819 plastic and plankton in the North Pacific central gyre. *Marine Pollution Bulletin*,
820 *42*(12), pp.1297-1300.
821 Nelms, S.E., Duncan, E.M., Broderick, A.C., Galloway, T.S., Godfrey, M.H., Hamann,
822 M., Lindeque, P.K. and Godley, B.J., 2015. Plastic and marine turtles: a review
823 and call for research. *ICES Journal of Marine Science*, *73*(2), pp.165-181.
824 Nilsen, F., Hyrenbach, K.D., Fang, J. and Jensen, B., 2014. Use of indicator chemicals to
825 characterize the plastic fragments ingested by Laysan albatross. *Marine*
826 *Pollution Bulletin*, *87*(1), pp.230-236.
827 Nishikida, K. and Coates, J., 2003. Infrared and Raman analysis of polymers. In: Lobo,
828 H., Bonilla, J.V. (editors) *Handbook of Plastics Analysis.* New York: Marcel
829 Dekker, Inc., pp.186-316.
830 Noda, I., Dowrey, A.E., Haynes, J.L. and Marcott, C., 2007. Group frequency
831 assignments for major infrared bands observed in common synthetic polymers. In:
832 Mark, J.E. (editor) *Physical Properties of Polymers Handbook*, New York:
833 Springer Science+Buisness Media, LLC, pp.395-406.
834 Peacock, A., 2000. *Handbook of Polyethylene: Structures, Properties, and Applications*.
835 New York: Marcel Dekker, Inc., pp.534.
836 Provencher, J.F., Bond, A.L., Avery-Gomm, S., Borrelle, S.B., Rebolledo, E.L.B.,
837 Hammer, S., Kühn, S., Lavers, J.L., Mallory, M.L., Trevail, A. and van Franeker,
838 J.A., 2017. Quantifying ingested debris in marine megafauna: a review and
839 recommendations for standardization. *Analytical Methods*, *9*(9), pp.1454-1469.
840 Rios, L.M., Moore, C. and Jones, P.R., 2007. Persistent organic pollutants carried by
841 synthetic polymers in the ocean environment. *Marine Pollution Bulletin*, *54*(8),
842 pp.1230-1237.
843 Rochman, C.M., Hoh, E., Hentschel, B.T. and Kaye, S., 2013. Long-term field
844 measurement of sorption of organic contaminants to five types of plastic pellets:
845 implications for plastic marine debris. *Environmental Science & Technology*,
846 *47*(3), pp.1646-1654.

847 Rotter, G. and Ishida, H., 1992. FTIR separation of nylon6 chain conformations:
848 Clarification of the mesomorphous and γcrystalline phases. *Journal of Polymer*
849 *Science Part B: Polymer Physics*, *30*(5), pp.489-495.
850 Ryan, P.G., Moore, C.J., van Franeker, J.A. and Moloney, C.L., 2009. Monitoring the
851 abundance of plastic debris in the marine environment. *Philosophical*
852 *Transactions of the Royal Society of London B: Biological Sciences*, *364*(1526),
853 pp.1999-2012.
854 Singh, B. and Sharma, N., 2008. Mechanistic implications of plastic degradation.
855 *Polymer Degradation and Stability*, *93*(3), pp.561-584.
856 Tomás, J., Guitart, R., Mateo, R. and Raga, J.A., 2002. Marine debris ingestion in
857 loggerhead sea turtles, Caretta caretta, from the Western Mediterranean. *Marine*
858 *Pollution Bulletin*, *44*(3), pp.211-216.
859 Unger, B., Rebolledo, E.L.B., Deaville, R., Gröne, A., IJsseldijk, L.L., Leopold, M.F.,
860 Siebert, U., Spitz, J., Wohlsein, P. and Herr, H., 2016. Large amounts of marine
861 debris found in sperm whales stranded along the North Sea coast in early 2016.
862 *Marine Pollution Bulletin*, *112*(1), pp.134-141.
863 Verleye, G.A., Roeges, N.P. and De Moor, M.O., 2001. *Easy Identification of Plastics*
864 *and Rubbers*. Shropshire: Rapra Technology Limited, pp.174.

865 Table 1. List of important vibration modes and mode assignments for the ATR FT-IR
866 spectra of eight of 16 polymers identified. The remaining eight polymers are in Table 2.
867 Absorption bands listed are representative of vibrations critical for polymer
868 identification. Please consult references for full lists of absorption bands. *Resolution
869 was 4 cm^{-1}. Letters can be cross referenced to bands shown in ATR FT-IR spectra in
870 Figure 1.

Polymer	Resin code	Chemical Structure	Absorption bands (cm^{-1}) used for identification*	Assignment	Reference in addition to this study
Polyethylene terephthalate (PETE)	1	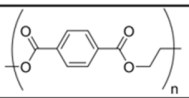	1713 (a) 1241 (b) 1094 (c) 720 (d)	C=O stretch C-O stretch C-O stretch Aromatic CH out-of-plane bend	Asensio et al., 2009; Verleye et al., 2001; Noda et al., 2007
High-density polyethylene (HDPE)	2		2915 (a) 2845 (b) 1472 (c) 1462 (d) 730 (e) 717 (f)	C-H stretch C-H stretch CH_2 bend CH_2 bend CH_2 rock CH_2 rock	Asensio et al., 2009; Noda et al., 2007; Nishikida & Coates, 2003
Polyvinyl chloride (PVC)	3		1427 (a) 1331 (b) 1255 (c) 1099 (d) 966 (e) 616 (f)	CH_2 bend CH bend CH bend C-C stretch CH_2 rock C-Cl stretch	Beltran & Marcilla 1997; Verleye et al., 2001; Noda et al., 2007
Low-density polyethylene (LDPE) or linear LDPE (LLDPE)	4	 R = H or alkyl (LLDPE), PE (LDPE)	2915 (a) 2845 (b) 1467 (c) 1462 (d) 1377 (e) 730 (f) 717 (g)	C-H stretch C-H stretch CH_2 bend CH_2 bend CH_3 bend CH_2 rock CH_2 rock	Asensio et al., 2009; Noda et al., 2007; Nishikida & Coates, 2003
Polypropylene (PP)	5		2950 (a) 2915 (b) 2838 (c) 1455 (d) 1377 (e) 1166 (f) 997 (g) 972 (h) 840 (i) 808 (j)	C-H stretch C-H stretch C-H stretch CH_2 bend CH_3 bend CH bend, CH_3 rock, C-C stretch CH_3 rock, CH_3 bend, CH bend CH_3 rock, C-C stretch CH_2 rock, C-CH_3 stretch CH_2 rock, C-C stretch, C-CH stretch	Asensio et al., 2009; Verleye et al., 2001; Noda et al., 2007
Polystyrene (PS)	6		3024 (a) 2847 (b) 1601 (c) 1492 (d) 1451 (e) 1027 (f) 694 (g) 537 (h)	Aromatic C-H stretch C-H stretch Aromatic ring stretch Aromatic ring stretch CH_2 bend Aromatic CH bend Aromatic CH out-of-plane bend Aromatic ring out-of-plane bend	Asensio et al., 2009; Verleye et al., 2001; Noda et al., 2007
Acrylonitrile butadiene styrene (ABS)	7	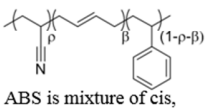 ABS is mixture of cis, trans, and vinyl isomers, linear and crosslinked	2922 (a) 1602 (b) 1494 (c) 1452 (d) 966 (e) 759 (f) 698 (g)	C-H stretch Aromatic ring stretch Aromatic ring stretch CH_2 bend =C-H bend Aromatic CH out-of-plane bend, =CH bend Aromatic CH out-of-plane bend	Verleye et al., 2001
Cellulose acetate (CA)	7	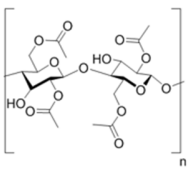	1743 (a) 1368 (b) 904 (c) 600 (d)	C=O stretch CH_3 bend Aromatic ring stretch or CH bend O-H bend	Iharco & Barros 2000; Verleye et al., 2001; Noda et al., 2007

871

Table 2. List of important vibration modes and mode assignments for the ATR FT-IR spectra for the remaining eight of 16 polymers identified. Absorption bands listed are representative of vibrations critical for polymer identification. Please consult references for full lists of absorption bands. *Resolution was 4 cm^{-1}. Letters can be cross referenced to bands shown in ATR FT-IR spectra in Figure 1.

Polymer	Resin code	Chemical Structure	Absorption bands (cm^{-1}) used for identification*	Assignment	Reference in addition to this study
Ethylene vinyl acetate (EVA)	7	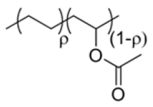	2917 (a) 2848 (b) 1740 (c) 1469 (d) 1241 (e) 1020 (f) 720 (g)	C-H stretch C-H stretch C=O stretch CH_2 bend, CH_3 bend C(=O)O stretch C-O stretch CH_2 rock	Asensio et al., 2009; Verleye et al., 2001
Latex	7	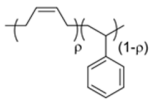 mixture of cis and trans, natural latex does not contain styrene copolymer	2960 (a) 2920 (b) 2855 (c) 1167 (d) 1447 (e) 1376 (f)	C-H stretch C-H stretch C-H stretch C=C stretch CH_2 bend CH_3 bend	Guidelli et al., 2011
Nitrile	7	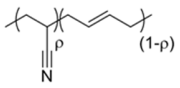 mixture of cis and trans	2917 (a) 2849 (b) 2237 (c) 1605 (d) 1440 (e) 1360 (f) 1197 (g) 967 (h)	=C-H stretch =C-H stretch CN stretch C=C stretch CH_2 bend CH_2 bend CH_2 bend =C-H bend	Coates, 2000; Verleye et al., 2001
Nylon (All polyamides)	7	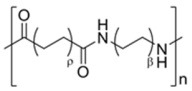 ρ and β vary from 0-12 based on monomer type	3298 (a) 2932 (b) 2858 (c) 1634 (d) 1538 (e) 1464 (f) 1372 (g) 1274 (h) 1199 (i) 687 (j)	N-H stretch CH stretch CH stretch C=O stretch NH bend, C-N stretch CH_2 bend CH_2 bend NH bend, C-N stretch CH_2 bend NH bend, C=O bend	Rotter & Ishida, 1992; Verleye et al., 2001; Noda et al., 2007
Polycarbonate (PC)	7	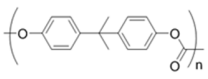	2966 (a) 1768 (b) 1503 (c) 1409 (d) 1364 (e) 1186 (f) 1158 (g) 1013 (h) 828 (i)	CH stretch C=O stretch Aromatic ring stretch Aromatic ring stretch CH_3 bend C-O stretch C-O stretch Aromatic CH in-plane bend Aromatic CH out-of-plane bend	Asensio et al., 2009; Verleye et al., 2001; Noda et al., 2007
Poly(methyl methacrylate) (PMMA or acrylic)	7	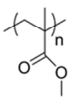	2992 (a) 2949 (b) 1721 (c) 1433 (d) 1386 (e) 1238 (f) 1189 (g) 1141 (h) 985 (i) 964 (j) 750 (k)	C-H stretch C-H stretch C=O stretch CH_2 bend CH_3 bend C-O stretch CH_3 rock C-O stretch CH_3 rock C-H bend CH_2 rock, C=O bend	Verleye et al., 2001
Polytetrafluoroethylene (PTFE) or fluorinated ethylene propylene (FEP)	7		1201 (a) 1147 (b) 638 (d) 554 (e) 509 (f)	CF_2 stretch CF_2 stretch C-C-F bend CF_2 bend CF_2 bend	Coates, 2000; Verleye et al., 2001
Polyurethane (PU)	7	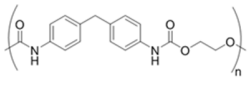	2865 (a) 1731 (b) 1531 (c) 1451 (d) 1223 (e)	C-H stretch C=O stretch C-N stretch CH_2 bend C(=O)O stretch	Asefnejad et al., 2011; Verleye et al., 2001; Noda et al., 2007

Table 3. Comparison of identifications of ingested plastic samples analyzed by attenuated total reflectance Fourier transform infrared spectroscopy (ATR FT-IR) and high-temperature size exclusion chromatography (HT-SEC) with infrared, differential refractive index, and multi-angle light scattering detection.

		HT-SEC Results			
Identification by ATR FT-IR	**Identification by HT-SEC**	RI peak magnitude	≠Average CH_3/ 1000 total C	*M_n (kg/mol)	*M_w (kg/mol)
PETE	¥PU				
HDPE	HDPE	-	11.2 ± 7	1.1	36.2
HDPE	HDPE	-	10.6 ± 8	26.6	161.2
HDPE	HDPE	-	6.2 ± 9	6.0	83.8
HDPE	HDPE	-	9.9 ± 15	5.0	32.8
HDPE	HDPE	-	5.7 ± 9	15.2	80.4
LDPE	LDPE	-	24.0 ± 5	42.5	148.3
LDPE	LDPE	-	35.8 ± 17	0.9	70.9
LDPE	LDPE	-	48.3 ± 16	2.5	65.6
LDPE	LDPE	-	25.7 ± 9	32.0	148.4
LDPE	LDPE	-	54.7 ± 12	33.2	197.1
PP	PP	-	338.7 ± 6	42.4	196.4
PP	PP	-	348.4 ± 18	4.7	58.6
PP	PP	-	303.5 ± 5	6.8	44.5
PS	PS	+	15.2 ± 23	21.7	52.5
PS	PS	+	35.2 ± 27	28.2	557.2
PS	PS	+	34.1 ± 51	137.6	281.7

≠Represents the relative methyl content of the polymer across the measured molar mass distribution. Error represents one standard deviation of the methyl content across all molar masses measured. Precision of molar mass measurements is ≤ 5% of reported value based on repeat injections of mass standards run during sample analyses.

¥Measured by XPS survey scan.

* Polymer number average (Mn) and mass average (Mw) molar masses determined by MALS detection.

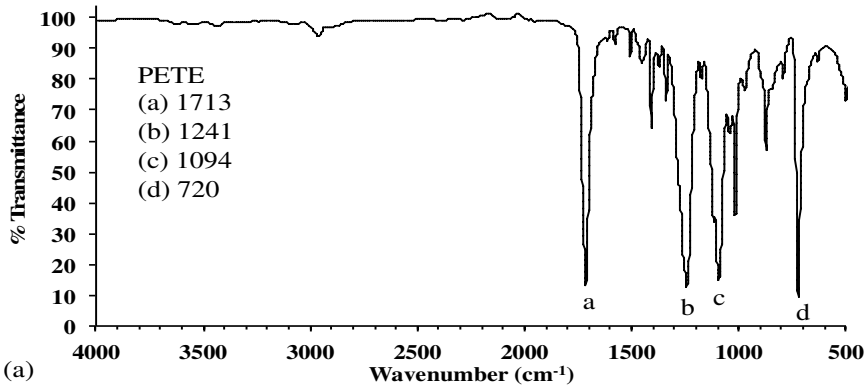
PETE
(a) 1713
(b) 1241
(c) 1094
(d) 720
% Transmittance
Wavenumber (cm-1)
a
b
c
d

(a)

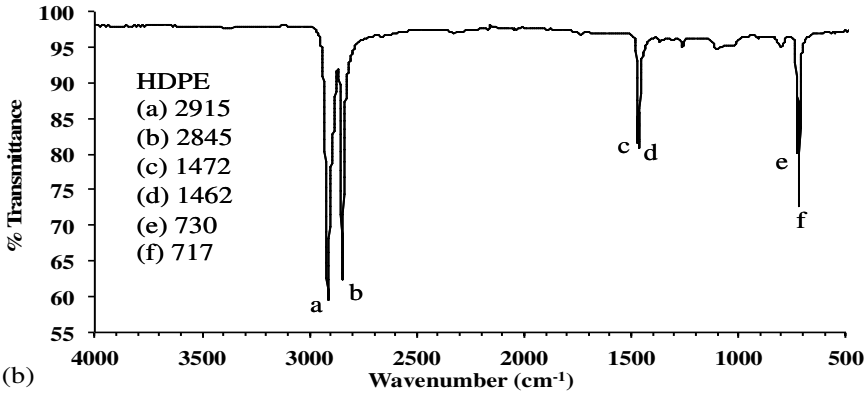
HDPE
(a) 2915
(b) 2845
(c) 1472
(d) 1462
(e) 730
(f) 717
% Transmittance
Wavenumber (cm-1)
a
b
c
d
e
f

(b)

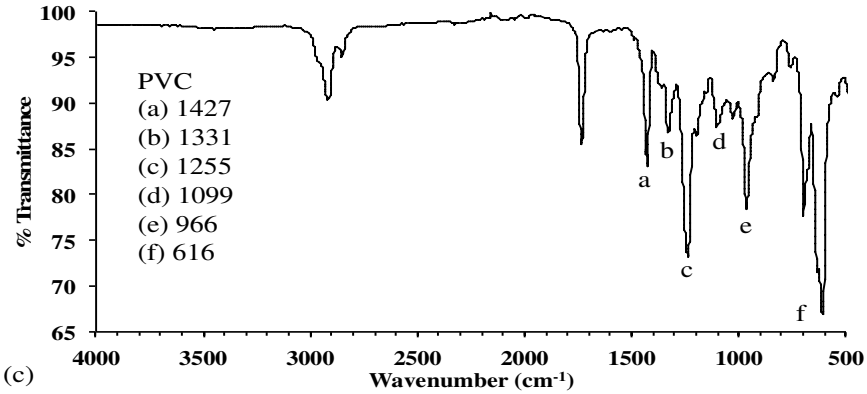
PVC
(a) 1427
(b) 1331
(c) 1255
(d) 1099
(e) 966
(f) 616
% Transmittance
Wavenumber (cm-1)
a
b
c
d
e
f

(c)

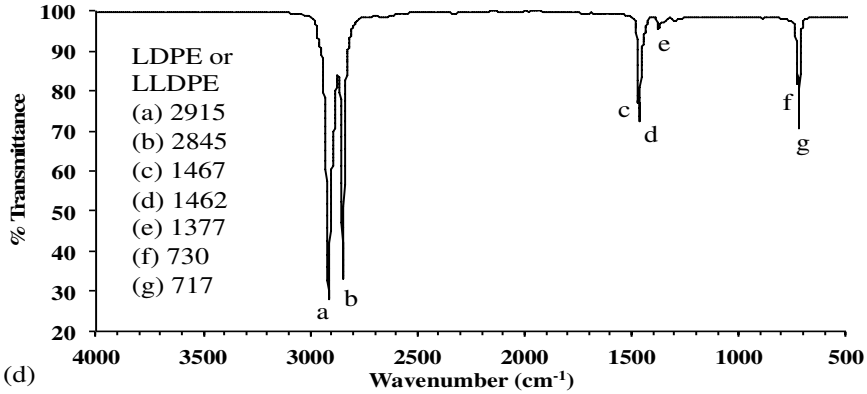
LDPE or
LLDPE
(a) 2915
(b) 2845
(c) 1467
(d) 1462
(e) 1377
(f) 730
(g) 717
% Transmittance
Wavenumber (cm-1)
a
b
c
d
e
f
g

(d)

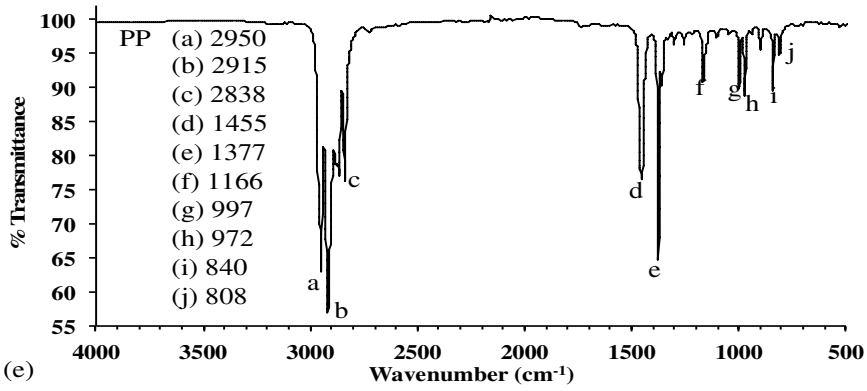
PP
(a) 2950
(b) 2915
(c) 2838
(d) 1455
(e) 1377
(f) 1166
(g) 997
(h) 972
(i) 840
(j) 808
% Transmittance
Wavenumber (cm-1)

(e)

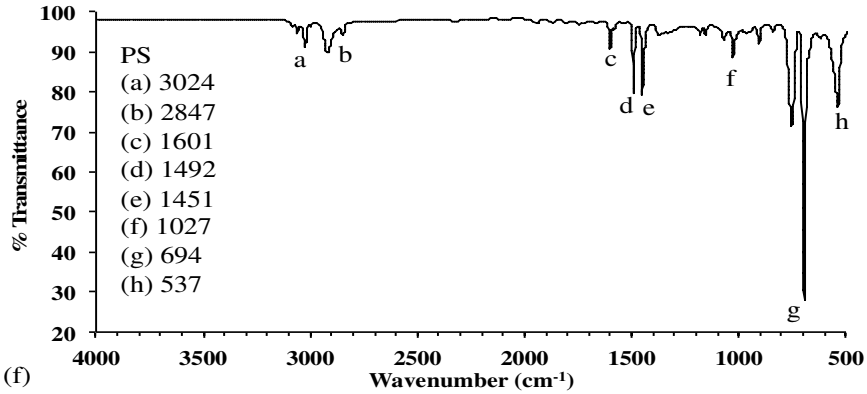
PS
(a) 3024
(b) 2847
(c) 1601
(d) 1492
(e) 1451
(f) 1027
(g) 694
(h) 537
% Transmittance
Wavenumber (cm-1)

(f)

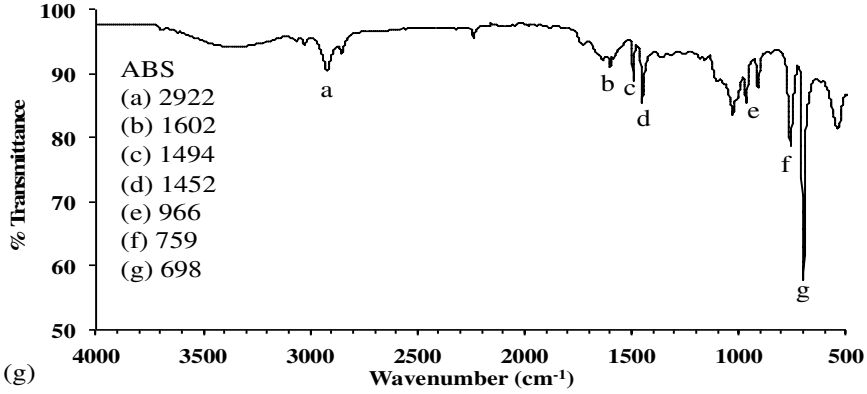
ABS
(a) 2922
(b) 1602
(c) 1494
(d) 1452
(e) 966
(f) 759
(g) 698
% Transmittance
Wavenumber (cm-1)

(g)

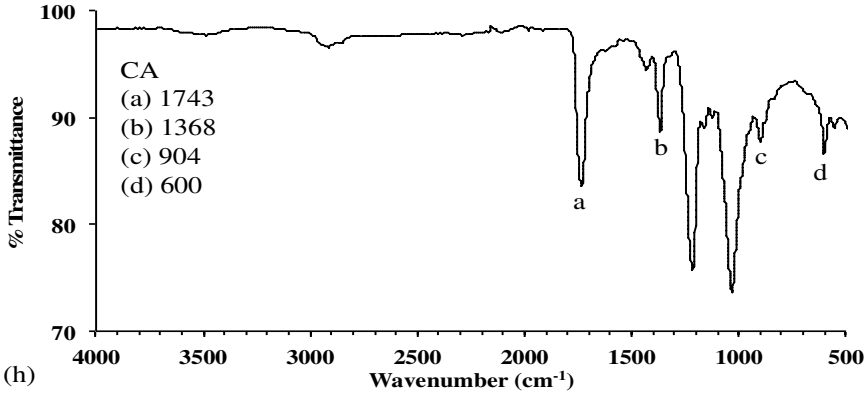
CA
(a) 1743
(b) 1368
(c) 904
(d) 600
% Transmittance
Wavenumber (cm-1)

(h)

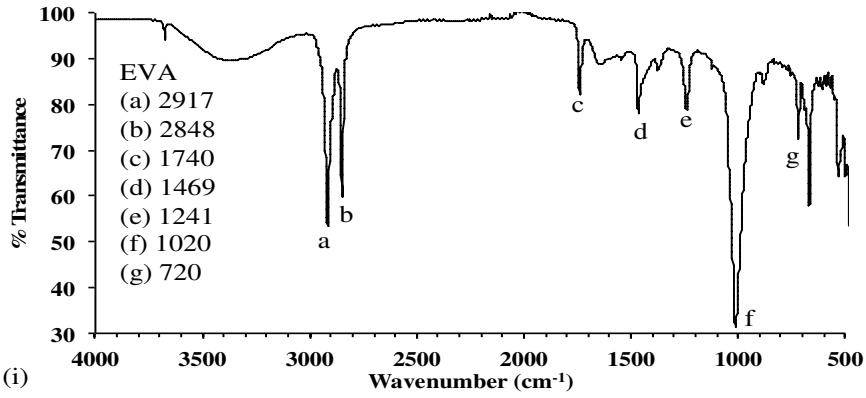
EVA
(a) 2917
(b) 2848
(c) 1740
(d) 1469
(e) 1241
(f) 1020
(g) 720
% Transmittance
Wavenumber (cm-1)

(i)

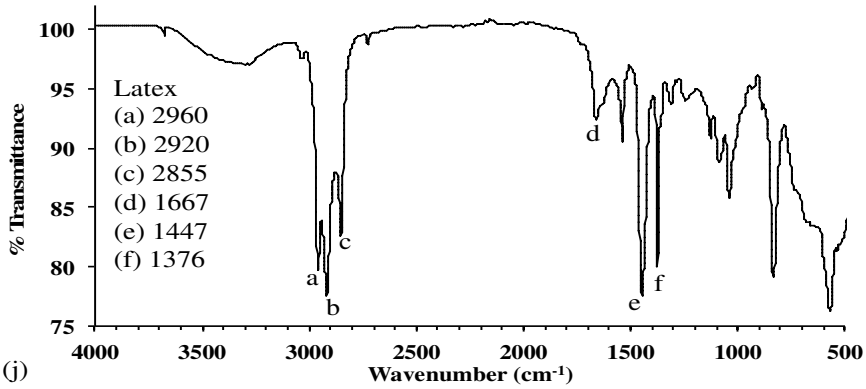
Latex
(a) 2960
(b) 2920
(c) 2855
(d) 1667
(e) 1447
(f) 1376
% Transmittance
Wavenumber (cm-1)

(j)

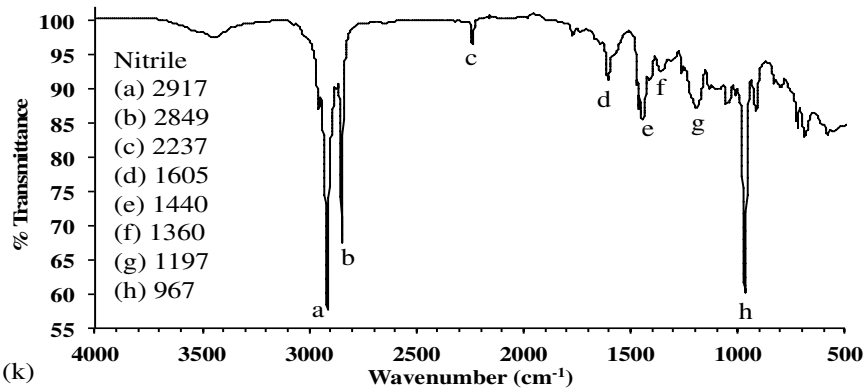
Nitrile
(a) 2917
(b) 2849
(c) 2237
(d) 1605
(e) 1440
(f) 1360
(g) 1197
(h) 967
% Transmittance
Wavenumber (cm-1)

(k)

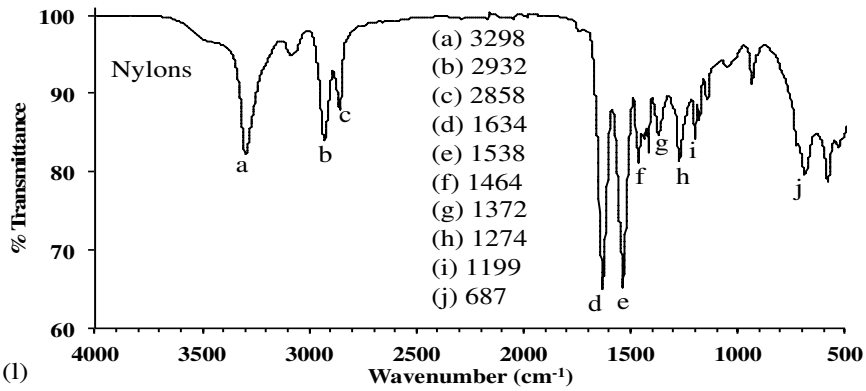
Nylons
(a) 3298
(b) 2932
(c) 2858
(d) 1634
(e) 1538
(f) 1464
(g) 1372
(h) 1274
(i) 1199
(j) 687
% Transmittance
Wavenumber (cm-1)

(l)

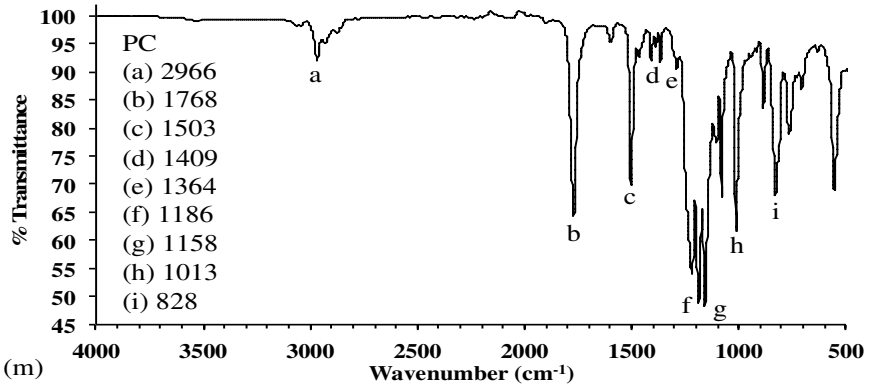
PC
(a) 2966
(b) 1768
(c) 1503
(d) 1409
(e) 1364
(f) 1186
(g) 1158
(h) 1013
(i) 828
% Transmittance
Wavenumber (cm-1)

(m)

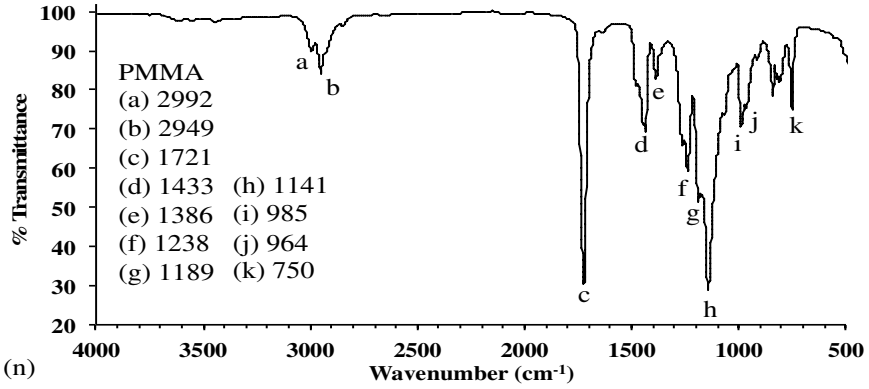
PMMA
(a) 2992
(b) 2949
(c) 1721
(d) 1433
(e) 1386
(f) 1238
(g) 1189
(h) 1141
(i) 985
(j) 964
(k) 750
% Transmittance
Wavenumber (cm-1)

(n)

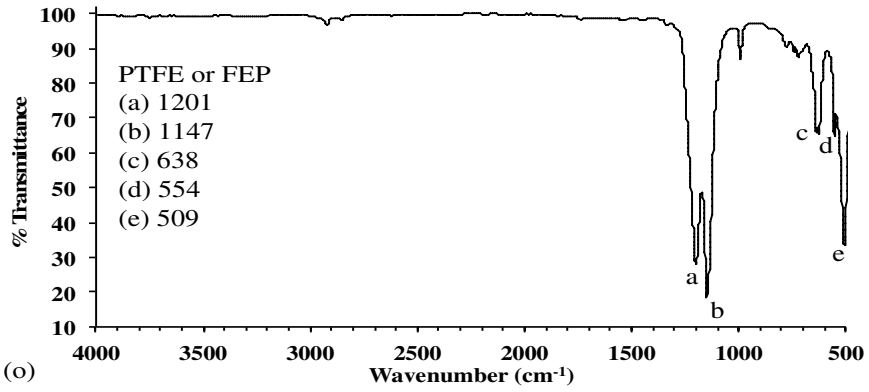
PTFE or FEP
(a) 1201
(b) 1147
(c) 638
(d) 554
(e) 509
% Transmittance
Wavenumber (cm-1)

(o)

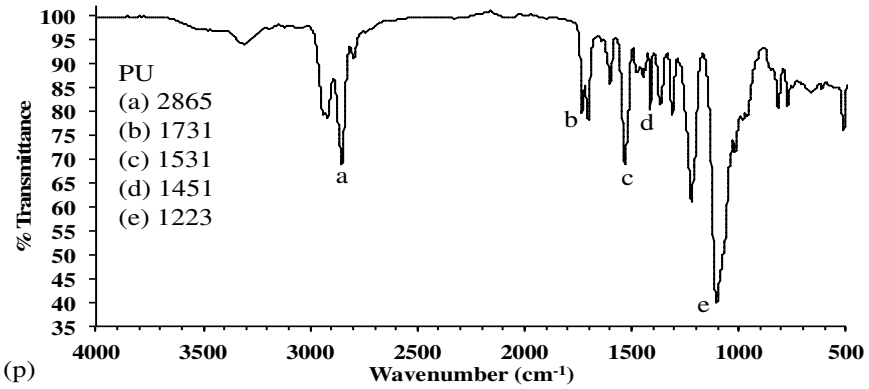
PU
(a) 2865
(b) 1731
(c) 1531
(d) 1451
(e) 1223
% Transmittance
Wavenumber (cm-1)

(p)

905 Figure 1. Spectra produced from plastic consumer goods labeled with resin codes of (a)
906 polyethylene terephthalate (PETE, #1), (b) high-density polyethylene (HDPE, #2), (c)
907 polyvinyl chloride (PVC, #3), (d) low-density polyethylene and linear low density
908 polyethylene (LDPE and LLDPE, #4), (e) polypropylene (PP, #5), and (f) polystyrene
909 (PS, #6) along with ten other polymers: (g) acrylonitrile butadiene styrene (ABS), (h)
910 cellulose acetate (CA), (i) ethylene vinyl acetate (EVA), (j) latex, (k) nitrile, (l) nylons,
911 (m) polycarbonate (PC), (n) poly(methyl methacrylate) (PMMA), (o)
912 polytetrafluoroethylene (PTFE) or fluorinated ethylene propylene (FEP), and (p)
913 polyurethane (PU) using ATR FT-IR. Letters represent characteristic absorption bands
914 (cm^{-1}) used to identify each polymer.

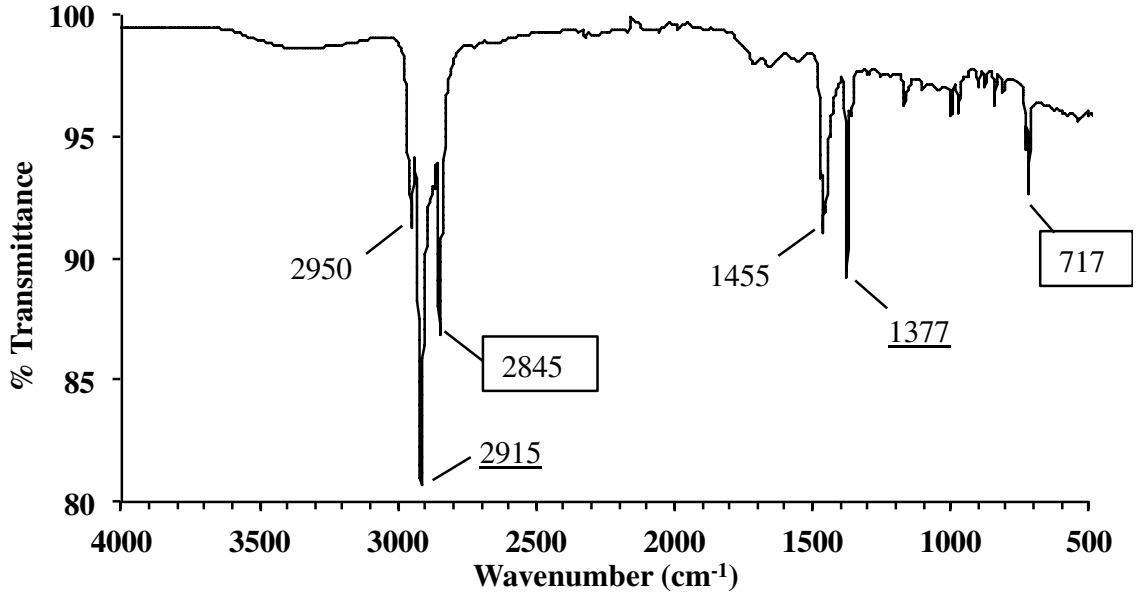

Figure 2. ATR FT-IR spectrum of an ingested plastic fragment assigned as a mixture of polyethylene (PE) and polypropylene (PP). Wavenumbers in boxes are characteristic of PE, underlined wavenumbers are characteristic of both PE and PP, and unmarked wavenumbers are characteristic of PP.

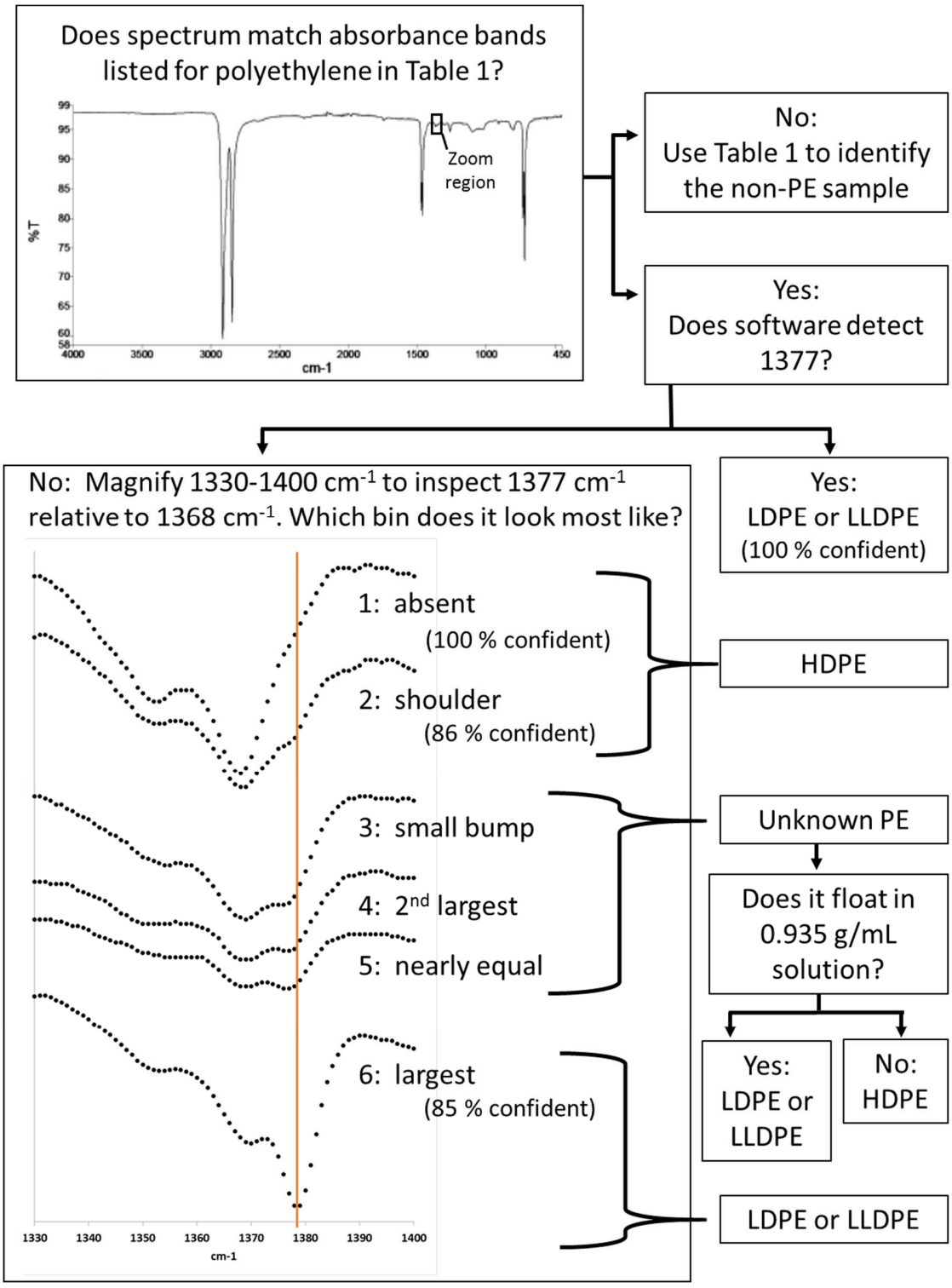

Figure 3. Decision flow chart for differentiating high-density polyethylene (HDPE), linear low-density polyethylene (LLDPE), and low-density polyethylene (LDPE) using ATR FT-IR spectra and float/sink tests.

925

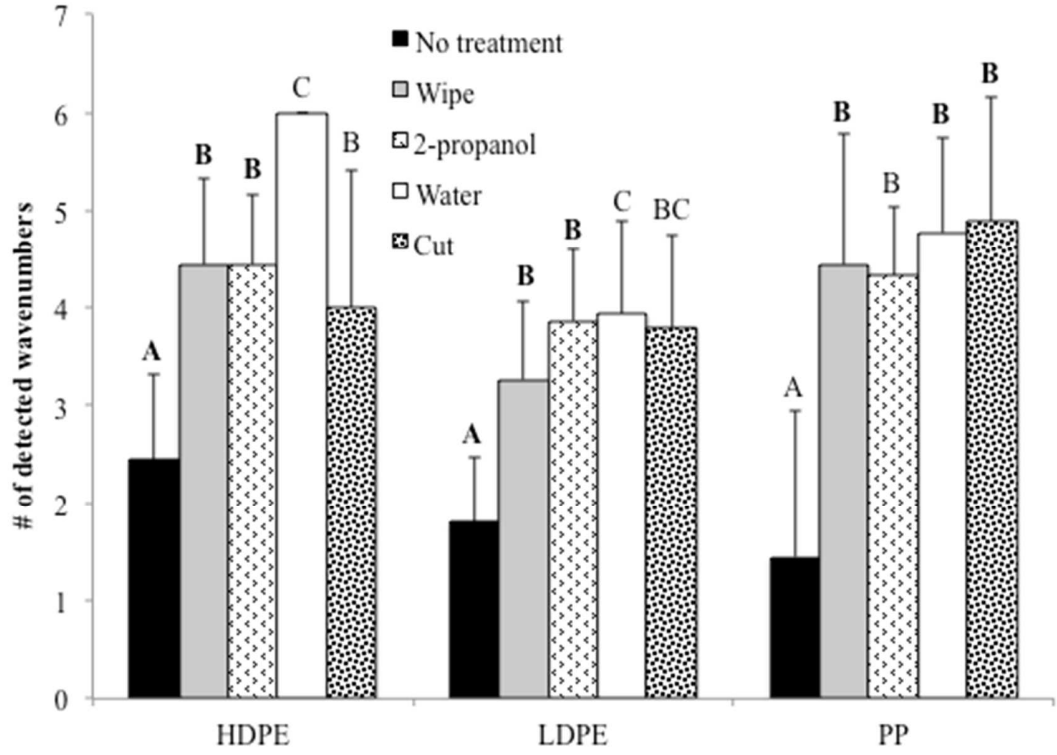

926

927 Figure 4. Mean and standard deviation of the number of detected wavenumbers for five
928 different cleaning methods on ingested high-density polyethylene (HDPE), low-density
929 polyethylene (LDPE), and polypropylene (PP) fragments. Different letters above bars
930 indicate significant differences among cleaning techniques within a polymer type ($p<0.05$
931 Wilcoxon signed-rank tests).

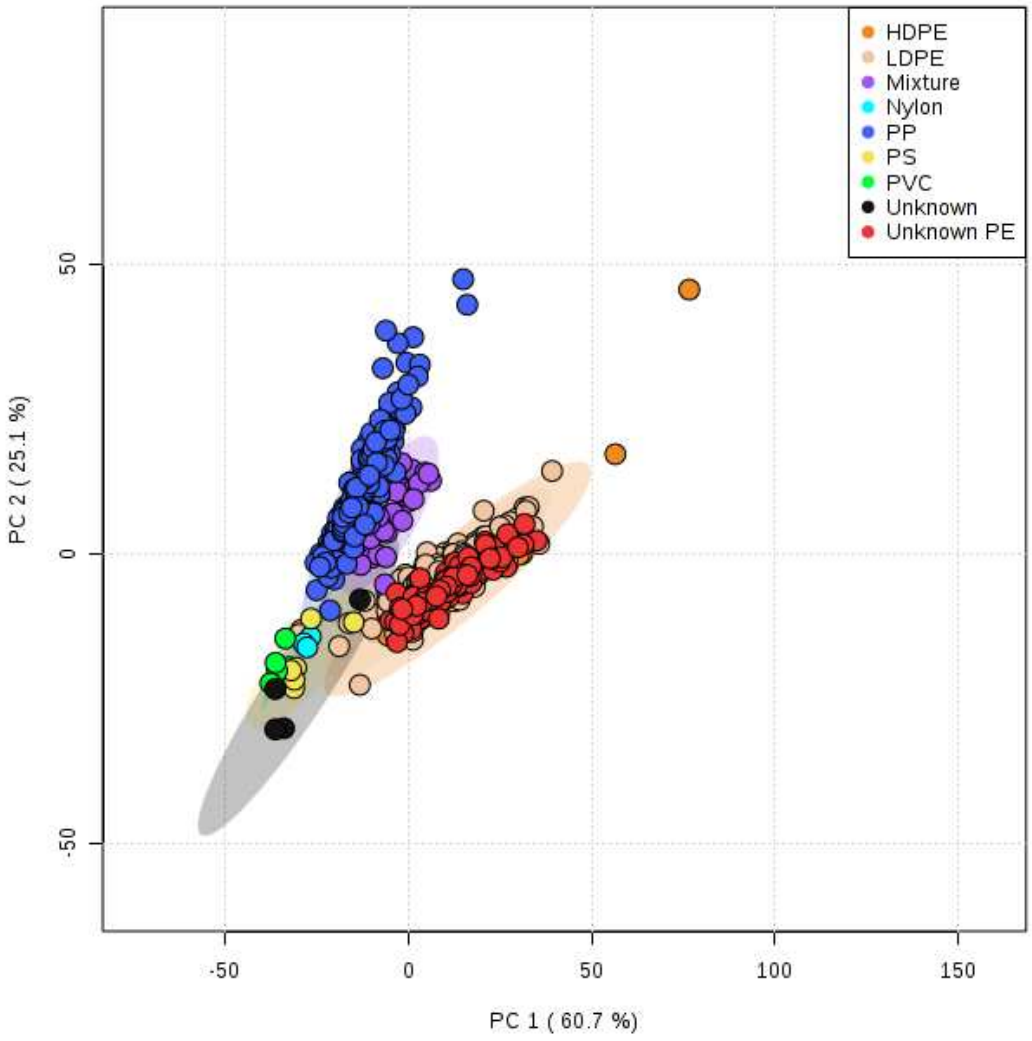

Figure 5. PCA ordination of spectra from ingested plastic samples identified as high-density polyethylene (HDPE, n = 58), polyvinyl chloride (PVC, n = 1), low-density polyethylene (LDPE, n = 310), polypropylene (PP, n = 270), polystyrene (PS, n = 7), nylon (n = 1), PE/PP mixture (n = 40), unknown PE (n = 106), and unknown (n = 4). Spectra of consumer good items representing PVC (n = 3) and nylon (n = 3) were also included. The amount of variation in the data explained by each principal component is shown in parentheses.

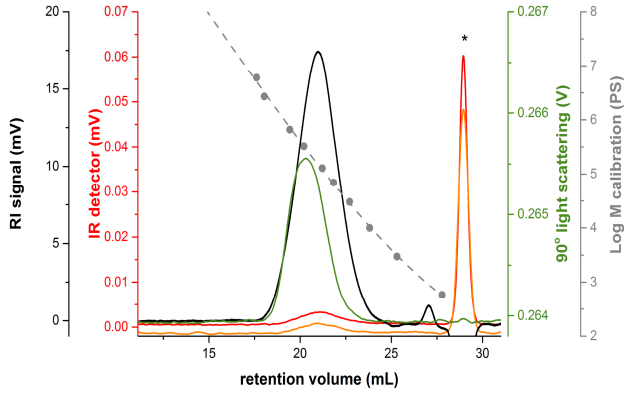

(a)

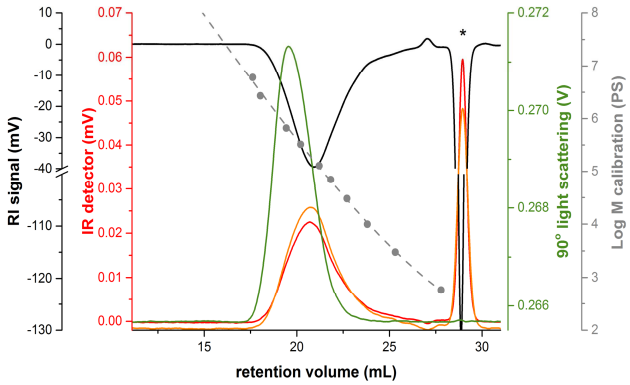

(b)

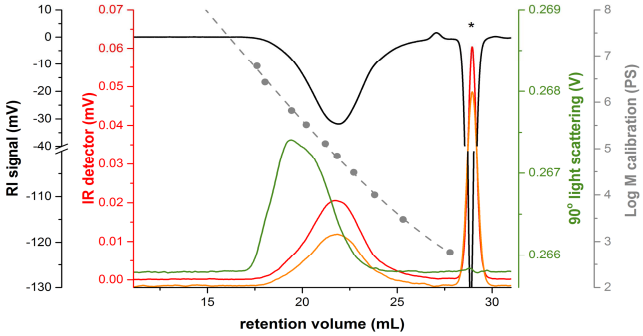

(c)

Figure 6. Representative HT-SEC chromatograms of samples run to confirm ATR-FTIR materials for ingested samples identified as (a) polystyrene (PS) (b) low-density polyethylene (LDPE) (c) high-density polyethylene (HDPE). The CH_3/1000 total C were measured by the ratio of the two IR signals, methyl stretching bands and alkyl stretching bands at 2950 cm^{-1} and (2800 to 3000) cm^{-1} (broad detector range), being represented by the orange and red traces, respectively. The asterisk (*) denotes an added flow rate marker, dodecane, used as an internal standard.

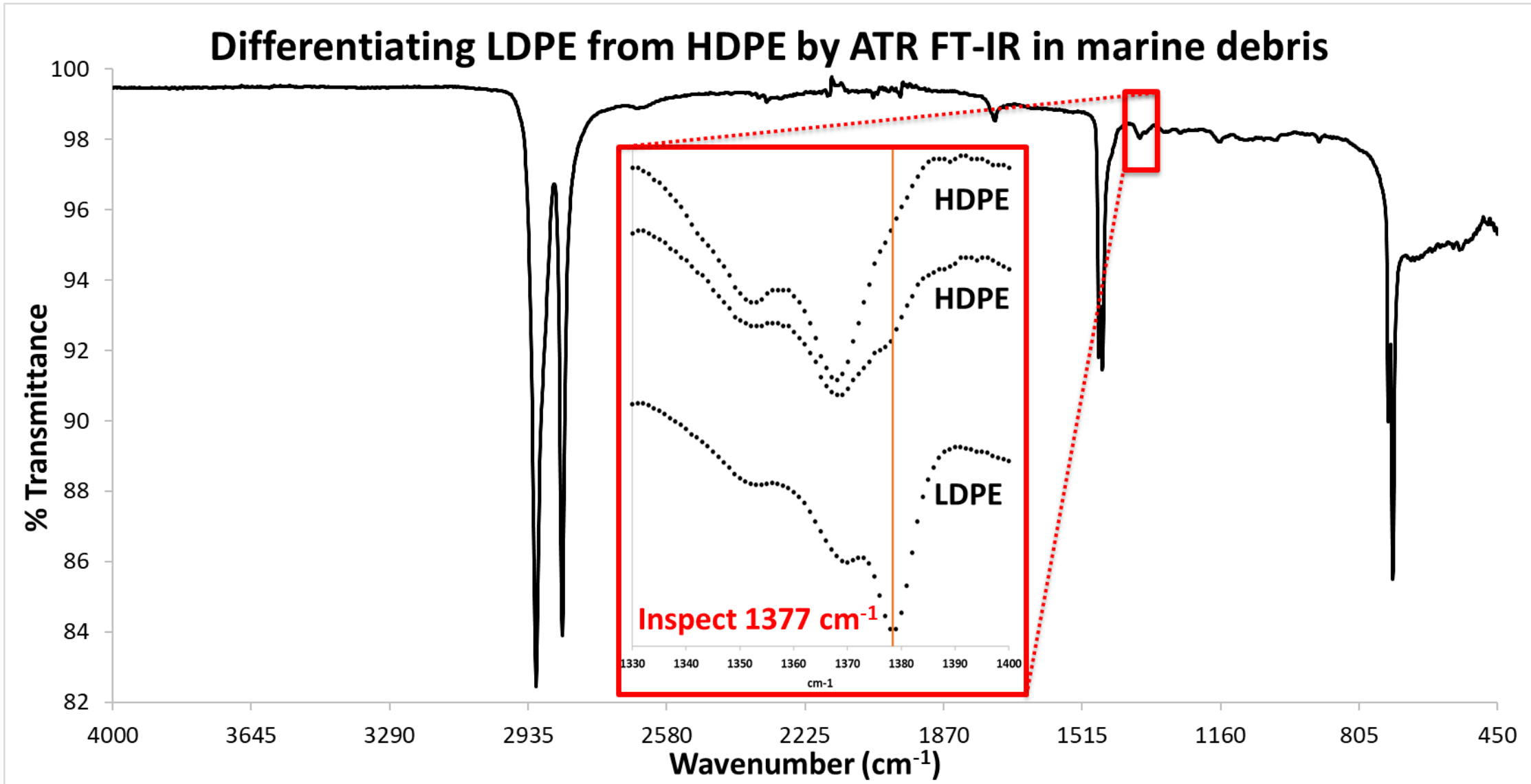
Differentiating LDPE from HDPE by ATR FT-IR in marine debris
% Transmittance
100
98
96
94
92
90
88
86
84
82
4000
3645
3290
2935
2580
2225
1870
1515
1160
805
450
Wavenumber (cm-1)
HDPE
HDPE
LDPE
Inspect 1377 cm-1
1330
1340
1350
1360
1370
1380
1390
1400
cm-1